12-2018

Morphometric Characteristics and Time to Hatch as Efficacious Indicators for Potential Nanotoxicity Assay in Zebrafish

Seyed-Mohammadreza Samaee
Urmia University, Iran

Nafiseh Manteghi
National Institute of Genetic Engineering and Biotechnology, Iran

Robert A. Yokel
University of Kentucky, ryokel@email.uky.edu

Mohammad Reza Mohajeri-Tehrani
Tehran University of Medical Sciences, Iran

Morphometric Characteristics and Time to Hatch as Efficacious Indicators for Potential Nanotoxicity Assay in Zebrafish

Digital Object Identifier (DOI)
https://doi.org/10.1002/etc.4266

Notes/Citation Information
Published in *Environmental Toxicology and Chemistry*, v. 37, issue 12.

Morphometric characteristics and time to hatch as efficacious indicators for potential nano-toxicity assay in zebrafish

Seyed-Mohammadreza Samaee[a]*; Nafiseh Manteghi[b]; Robert A. Yokel[c], Mohammad Reza Mohajeri-Tehrani[d]

[a]Aquatic Lab, Department of Food Hygiene and Quality Control, Faculty of Veterinary Medicine, Urmia University, Urmia 165, Iran;

[b]National Institute of Genetic Engineering and Biotechnology, Tehran, Iran;

[c]Department of Pharmaceutical Sciences, University of Kentucky, Lexington, KY, US

[d]Endocrinology & Metabolism Research Institute, Tehran University of Medical Sciences, Tehran 14114 13137, Iran

*Corresponding author: Seyed-Mohammadreza Samaee; Tel: +98-044-32770508; E-mail: seyedmohammadreza.samaee@gmail.com & mohammadreza_samaee@yahoo.com; ORCID: 0000-0002-9104-0299

Running head: Zebrafish morphology & hatch time indicate nanotoxicity

Abstract. Although the effects of nanosized titania ($nTiO_2$) on hatching events (change in hatching time and total hatching) in zebrafish have been reported, additional consequences of $nTiO_2$ exposure, i.e. the effects of $nTiO_2$-induced changes in hatching events and morphometric parameters on embryo-larvae development and survivability have not been reported. To address this knowledge gap, embryos 4 h post-fertilization were exposed to $nTiO_2$ (0, 0.01, 10, and 1000 μg/mL) for 220 h. Hatching rate (HR; 58, 82, and 106 hours postexposure [hpe]), survival rate (SR; 8 times from 34 to 202 hpe), and 21 morphometric characteristics (MCs; 8 times from 34 to 202 hpe) were recorded. Total hatching (HR at 106 hpe) was significantly and positively correlated to SR, but there was no direct association between $nTiO_2$-induced change in hatching time (HR at 58 and 82 hpe) and SR. MCs were significantly correlated to HR at 58, 82, and 106 hpe, suggesting the $nTiO_2$-induced change in hatching time can affect larval development. The MCs that were associated with change in hatching time were also significantly correlated to SR, suggesting an indirect significant influence of the $nTiO_2$-induced change in hatching time on survivability. These results show a significant influence of $nTiO_2$-induced change in hatching events on zebrafish embryo-larvae development and survivability. They also show that morphometric maldevelopments can predict later-in-life consequences (survivability) of an embryonic exposure to $nTiO_2$. This suggests that zebrafish can be sensitive biological predictors of $nTiO_2$ acute toxicity.

Keywords: Hatchability, Morphometric characteristics, NM-105, Survivability, Zebrafish embryo-larvae

1. Introduction

47 Metal oxide nanoparticles (MNP), similar to other particles at the nanoscale (1-100 nm
48 [Colvin 2003]), have unique physicochemical properties compared to parent metals that can
49 induce adverse and unique effects in aquatic organisms (Lovern and Klaper 2006; Moore 2006;
50 Griffitt et al. 2009). MNPs are considered to be an emerging class of environmental pollutants
51 (Service 2004). MNPs possess multiple mechanisms of toxicity that can affect multiple levels of
52 biological organization (Metcalfe et al. 2009).

53 Nano-TiO_2 ($nTiO_2$) is a MNP that has frequent use and widespread industrial applications
54 (Jovanović et al. 2011b). As such, there is the potential for environmental contamination and
55 exposure to $nTiO_2$ (Hall et al. 2009). $nTiO_2$ is a suspected group 2B human carcinogen
56 (Jovanović et al. 2011b). In response to the concerns mentioned above, many studies have
57 investigated the adverse effects of $nTiO_2$ aqueous suspensions on the environment, wildlife, and
58 human health (Menard et al. 2011).

59 The impact of $nTiO_2$ exposure on zebrafish hatching events has been investigated and
60 reported as premature (Kovrižnych et al. 2013; Ma and Diamond 2013; Fouqueray et al. 2013;
61 Samaee et al. 2015) or delayed hatching (Yeo and Jo 2007; Xu et al. 2012). There are also other
62 studies (e.g. Jovanović et al. 2015; Clemente et al. 2014; Wang et al. 2014; Yan et al. 2014) in
63 which viability parameters (e.g. hatching events and/or survivability) have been considered to
64 characterize $nTiO_2$-induced toxicity. These reports warrant further study to identify aspects of
65 $nTiO_2$-induced changes in hatching events in relation to zebrafish embryo-larvae development
66 and survivability.

67 Phenotypic characteristics are not only the most common, applicable and robust
68 responses assessed in zebrafish embryo and larvae toxicology (e.g. see Bar-Ilan et al. 2009) but
69 phenotypic characterization is also very amenable to automation and high throughput (Vogt et al.

2009; Liu et al. 2012). In previous studies, the phenotypic analyses of $nTiO_2$-induced defects have been performed based upon morphological characteristics (qualitative signs that include dorsal curvature, kinked tail, edema, elongated heart, and others) (Yeo and Kang 2009; Bar-Ilan et al. 2009; Yeo and Kim 2010; He et al. 2014; Wang et al. 2014; Yan et al. 2014). However, generating quantitative data from morphometric characteristics (MC) has been largely ignored or under-used in toxicology assays.

The current study objectives were: 1) to test the hypothesis whether the viability parameters such as hatching events and survivability, as well as morphometric characteristics can characterize the $nTiO_2$-induced toxicity in zebrafish embryo-larvae, 2) to evaluate if $nTiO_2$-induced changes in hatching events (as sub-lethal endpoints) are significantly correlated to embryo-larvae morphometric alterations (as another sub-lethal endpoint that is also accounted for as a criterion for larval development) and survivability (as an acute endpoint), both during $nTiO_2$ exposure and after $nTiO_2$ depuration, and 3) to test the hypothesis that $nTiO_2$-induced changes in sub-lethal endpoints (i.e. hatching events and MCs) can predict later-in-life consequences of zebrafish embryonic/larval exposure.

2. Materials and methods

2.1. Zebrafish source and housing

Wild-type zebrafish were purchased from a local supplier in the North of Iran (local suppliers are the only source of wild-type zebrafish here), and maintained in a semi-static system. They were housed in covered glass tanks (50 cm L × 30 cm W × 30 cm H). The tanks were aerated and equipped with a sponge filtration unit, a 150 W submersible heater (Atman®, China), and a 6 W white light (DGL-1540 S-M, Bohem Ltd. Co., China) located on the lid of the

93 tank. Municipal (tap) water was dechlorinated and adjusted to 28 ºC after filtration through an
94 active carbon filter (a fully submersible sponge filter [WP, 1150F, Sobo®, China] in which its
95 sponge was replaced with activated carbon [C-300, Aleas®, China]). After filtration, water was
96 conditioned with 240 mg/L rock salt + 60 mg/L sea salt (Westerfield 2000).
97
98 2.2. Zebrafish maintenance
99 After determination of sex (Braunbeck and Lammer 2006), males and females were
100 segregated and housed on a 14:10 h light:dark cycle (9:00 a.m. on, 11:00 p.m. off) (Westerfield
101 2000). Adult zebrafish were fed a combination of several types of food depending on their
102 development stage and age (flake food Vitakraft® and TetraMin®, Germany; and BioMar and
103 live food - brine shrimp Nauplii) to satiation twice a day (Lawrence 2007). Zebrafish larvae from
104 day 2 (34 hours postexposure [hpe]) to 6 (130 hpe) grew on yolk nutrients and were not fed,
105 while from day 6 to day 9 (202 hpe) larvae were fed *Paramecium spp*. twice daily as described
106 by Varga (2011).
107
108 2.3. Zebrafish spawning and embryo collection
109 Healthy males and females (6–18 months old) were segregated one week before
110 breeding. Two males and 3 females were transferred to mating tanks (FH-101, Guangdong boyu
111 aquarium industries Co., Ltd, China) late in the afternoon the day before spawning. Males and
112 females were housed in different chambers, separated by a transparent plastic divider in the
113 mating cage. At 9:00 h the divider was removed and the zebrafish mated and spawned. Embryos
114 were siphoned from the bottom of the spawning tank into a Petri dish containing conditioned
115 system water (see section 2.1). Methylene blue (0.5 mg/L) was added to the embryo rearing

116 medium to prevent fungi growth. Live embryos were collected at ~ 2 hours post-fertilization
117 (hpf; blastula stage) (Fouqueray et al. 2013).
118
119 2.4. The $nTiO_2$ nanopowder
120 Degussa P-25 titanium dioxide nanopowder (NM-105) was obtained from Evonik
121 Industries (Frankfurt am Main, Germany). It is a mixture of ~80% anatase and ~20% rutile
122 crystals with an average primary particle size of 21 nm (Ohno et al. 2001; Evonik Industries
123 2007). NM-105 is a standard $nTiO_2$ reference material deposited in the European Commission
124 Joint Research Centre (Rasmussen et al., 2014).
125
126 2.5. P-25 $nTiO_2$ suspension preparation
127 A known mass of P-25 was added to a known volume of dispersant (autoclaved [Paterson
128 et al. 2011] egg water: distilled water containing sea salt [60 mg/L], pH 7.2 [Westerfield 2000])
129 to produce a 1000 µg/mL stock suspension. The suspension was agitated using a probe sonicator
130 (Hielscher UP400S, Germany) at 320 W (0.5 cycle, amplitude 85%) in an ice bath for at least 30
131 min followed by bath sonication (Elmasonic S100H, Germany) for 15 min. The suspension was
132 used immediately after preparation. Working solutions of other concentrations were prepared by
133 stepwise dilution of stock suspension with egg water. The Ti^{4+} (ionic portion of $nTiO_2$), was also
134 quantified based on Samaee et al. (2015).
135
136 2.6. $nTiO_2$ characterization
137 The characterization was made at two times: 1) immediately after preparation of the
138 $nTiO_2$ suspension (before waterborne exposure) and 2) 24 h after preparation of the $nTiO_2$

139 suspension (after waterborne exposure) (Kim et al. 2014). Suspension samples at both time
140 points were collected from the center of the water column (Clemente et al. 2014) and the
141 undisturbed top layer (Dalai et al. 2012). Samples were analyzed, as described below, at room
142 temperature. Experiments were carried out in triplicate to calculate the standard deviation (Dalai
143 et al., 2012).

144 $nTiO_2$ morphology (Zhu et al., 2008) and primary particle diameter were determined by
145 transmission electron microscopy (TEM). Twenty µL of $nTiO_2$ (100 ppm) was pipetted onto
146 carbon-coated copper grids (Formvar carbon coated grid Cu Mesh 300, EMS, USA) then dried in
147 a laminar flow hood for 24 h. The microscope (Zeiss EM10C, USA) was operated in bright field
148 mode. Specimens were observed with a Bosch camera (Germany) at an accelerating voltage of
149 100 kV. Particle size distribution (PSD) was statistically computed from 107 particles viewed in
150 a series of images using ImageJ software 1.48 (Wayne Rasband, National Institutes of Health,
151 USA [http://imagej.nih.gov/ij]) (Kim et al. 2014; He et al. 2014). The PSD, average
152 hydrodynamic diameter, polydispersity index (PDI), and surface charge (zeta potential) were
153 characterized by dynamic light scattering (DLS) (Zetasizer Nano ZS instrument [Malvern
154 Instruments, Zen 3600, UK]). One mL of 1 µg/mL $nTiO_2$ suspension was analyzed using a
155 refractive index of nR=2.5 (https://refractiveindex.info/?shelf=main&book=Ti&page=Johnson)
156 at 25 °C. Egg water without particles was the control. Three independent measurements were
157 taken with 3 readings per time point (at 0 and 24 h post suspension preparation), each reading
158 consisting of six runs of 10 s duration (Faria et al. 2014).

159 The concentration (colloidal stabilities) of the 0.01, 10, and 1000 µg/mL suspensions
160 were estimated by visible spectroscopy using a UV/Vis/Nir Spectrophotometer (lambda 950,
161 PerkinElmer Inc., USA) (Paterson et al. 2011). In brief, $nTiO_2$ standards were prepared as 10, 20,

33, 50, and 100-fold dilutions of the stock suspension in egg water and re-sonicated for 10 s. The standards were used to generate a linear concentration curve at the wavelength of maximum absorbance (321 nm) for the Degussa P-25 material suspended in egg water. Sample absorbance was used to estimate its concentration from the standard curve.

Attenuated total reflectance Fourier-transform infrared spectroscopy (ATR-FTIR) characterization of $nTiO_2$ was carried out in the 650–4000 cm^{-1} range, with a resolution of 4 cm^{-1} at room temperature using a Nexus 470 FTIR spectrometer (Thermo-Nicolet, USA).

2.7. Exposure procedure (or protocol)

A static renewal fish embryo toxicity test was performed with three $nTiO_2$ concentrations (0.01, 10, and 1000 µg/mL), Ti^{4+} (0.0001 µg/mL), and a negative control (egg water). This concentration range includes 1) the LC_{50} for 96 h acute fish toxicity and the EC_{50} in the fish embryo test for 73 chemicals (Lammer et al. 2009), 2) the predicted realistic and high emission environmental concentrations for nano-$nTiO_2$ in water (0.0007 and 0.016 µg/mL, respectively) (Mueller and Nowack 2008), and 3) extends both below and above the concentration range of prior studies of zebrafish exposed to water-borne $nTiO_2$ (Clemente et al. 2014; Wang et al. 2014; Yan et al. 2014). Exposure procedure of embryo-larvae was carried out based on Samaee et al. (2015).

Embryo-larvae were exposed to $nTiO_2$ from day 0 (at 4 hpf [the sphere stage of the blastula stage – Yan et al. 2014]) to day 6 (incomplete yolk resorption). This time period normally spans from egg fertilization to the time of hatch and then to yolk resorption of the sac fry following a well characterized set of developmental stages. The embryo-larvae grew on yolk nutrients, and were not fed.

On day 6 (130 hpe) the exposure solution (egg water containing Ti^{4+} or $nTiO_2$) was replaced with egg water for a depuration period of 4 days (see studies of Paterson et al. [2011] on Japanese medaka). From day 6 to day 9 (202 hpe) larvae were fed *Paramecium* spp. twice daily (Varga 2011). On day 5 to 6 the digestive tract opens and digestive enzymes are secreted, suggesting the larval fish can begin exogenous feeding even though the yolk sac is not yet completely depleted (Holmberg et al. 2004). Culture medium was completely changed after each feeding.

Plates were examined at 34, 58, 82, 106, 130, 154, 178, and 202 hpe. These times correspond with known developmental stages: 34 hpe (embryonic stage); 58 hpe (hatching); 82 hpe (yolk sac larva/eleutheroembryos [stage between hatching and start of external feed intake] [Oliver et al. 2015]); 106 hpe (gas bladder inflation [Goolish and Okutake 1999], 4 mm free swimming larva [Chen et al. 2011], and opening of gut end to end [Wilson 2012]); 130 hpe (initiation of exogenous feeding while yolk sac is not yet completely depleted [Holmberg et al. 2004]); and 157 hpe (complete depletion of yolk sac [Jardine and Litvak 2003; Wilson 2012]) (Figure 1).

At each time point, the following were recorded: i) HR, ii) mortality rate (dead embryo-larvae were removed), and iii) morphometries of four embryo-larvae specimen (for embryo-larvae biometry). The exposure solution was completely changed at each time point (Kim et al. 2014).

2.8. Recording of endpoints

2.8.1. Morphometric characteristics (MCs)

207 Four embryo-larvae specimens were randomly taken at each sampling time from each
208 treatment. They were fixed in 10% neutral buffered formalin for 24 h (Vicario-Parés et al. 2014).
209 Photomicrographs were taken of the fixed specimens (Figure 2) using a stereomicroscope
210 (Zeiss) equipped with a digital camera (Carl Zeiss Inc.). Digital images were processed with
211 Image J 1.48 to quantify embryo-larvae morphometric characteristics (Figure 3).
212
213 2.8.2. Calculation of embryo-larvae viability parameters
214 Viability calculations included the following: 1) Hatching rate, HR=(Hatched embryos
215 /Total number of cultured embryos)×100) at 58, 82, and 106 hpe; and 2) survival rate, SR=(Alive
216 larvae/Total number of cultured embryo-larvae)×100) at 34, 58, 82, 106, 130, 154, 178, and 202
217 hpe. HR and SR descriptive statistics (mean, standard deviation [SD], and coefficient of variation
218 [CV]) were calculated. LC_{50} values and their 95% confidence intervals for $nTiO_2$ exposure\were
219 assessed by Probit analysis using SPSS IBM (version 20; SPSS Inc., Chicago, IL, USA).
220
221 2.9. Statistical analysis
222 Data normality was tested by the Anderson-Darling method. Univariate analysis of
223 variance (ANOVA; followed by Duncan's multiple range post hoc test) and cluster analysis
224 (followed by multivariate analysis of variance [MANOVA]) were used to test for differences
225 among treatment groups for HR, SR, and MCs. A *p*-value of 0.05 was accepted for statistical
226 significance. Simple regression models were formulated to characterize MCs and the endpoints
227 that are correlated to HR and SR. A *p*-value of <0.002 was accepted for determining the level of
228 significance for the regression analysis; considered to be the statistical significance threshold
229 after applying the Bonferroni's adjustment for the critical value of $p<0.05$ to minimize the chance

of type I statistical error. All statistical analyses were performed using IBM SPSS (version 20; SPSS Inc., Chicago, IL, USA), and Excel 2010 (Microsoft Corporation, Redmond, WA, USA).

3. Results

3.1. $nTiO_2$ characteristics

TEM images of $nTiO_2$ are shown in Figure 4a and f. The $nTiO_2$ particles were approximately polyhedral with rounded borders with relatively uniform size distribution. Their diameter (mean [SD] = 22 [5] nm), was consistent with the manufacturer-reported value (21 nm; see section 2.4).

The intensity-averaged hydrodynamic diameter distribution of $nTiO_2$ dispersed in egg water is shown in panels b and g of Figure 4. The average particle diameter (Z-average) and PDI of the $nTiO_2$ immediately after preparation of the $nTiO_2$ suspension (Figure 4b), were 197 [1] nm and 0.16 [0.01] (mean [SD]) (less than 0.25, indicating that the suspension was monodispersed without significant aggregation [Li et al. 2013]). The parameters 24 h after preparation were 192 [6] nm and 0.15 [0.02] (mean [SD]) (Figure 4g).

Zeta potential was 34 [1] (mean [SD]) mV (Figure 4e), immediately after preparation of the $nTiO_2$ suspension and 16[0] (mean [SD]) mV (Figure 4j), 24 h after its preparation. The zeta potential was quite high immediately after $nTiO_2$ suspension preparation (Figure 4e) what indicates a low tendency to agglomeration. The decrease of this value 24 h later (Figure 4j) indicates an increased tendency to agglomerate.

Visible spectrophotometry indicated a significant decrease in the concentration of dispersed $nTiO_2$ from 0 to 24 h after its preparation; the $nTiO_2$ concentration of 500 μg/mL immediately after suspension preparation decreased to 4 0 μg/mL after 24 h. This is not

surprising, because in suspension, $nTiO_2$ tends to form large particles and most of the agglomerates settle out (Adams et al. 2006). Dr. José M. Navas (Department for the Environment, INIA, Spain) suggested that this does not indicate a change in the $nTiO_2$ concentration in the entire $nTiO_2$ dispersion, but that $nTiO_2$ is not present in the water column (personal communication 2017). Chen et al. (2011) suggest that although sedimentation occurs, the embryo-larvae are constantly exposed to the $nTiO_2$ aggregates during the bioassay because the embryo-larvae are mostly located on the bottom of microplates before they can freely swim.

The FTIR spectra of $nTiO_2$ (Figure 4k-m) clearly shows two bands. The first, observed at 3250 cm^{-1}, corresponds to the stretching vibration of the hydroxyl group (O-H) of the $nTiO_2$. The second around 1630 cm^{-1} corresponds to bending modes of water Ti-OH (Nadica et al. 2006; Mugundan et al. 2015; León et al. 2017). The FTIR spectra at 0 (Figure 4k), 12 (Figure 4l), and 24 h (Figure 4m) after $nTiO_2$ suspension preparation are the same, suggesting no modification of the NP surface chemistry in these 24 h. For the results of titanium analysis, see Samaee et al. (2015).

3.2. Effect of Ti^{+4} on HR, SR, and MCs

To determine if there was any contribution of the soluble fraction to the $nTiO_2$ response, embryos-larvae were exposed to the 0.0001 µg/mL Ti^{+4}, the concentration of the soluble fraction of $nTiO_2$. No significant difference of HR, SR, and MC (>0.05) was detected when comparing embryo-larvae exposed to Ti^{+4} to controls (Table 1).

3.3. Differences among treatments concerning HR

275 $nTiO_2$ had a significant effect on HR at 58 hpe (Figure 5a), but not 82 hpe (Figure 5b), or
276 106 hpe (Figure 5c). Cluster analysis, based on descriptive statistics (mean, SD, and CV) of HR
277 (Figure 5j), categorized the four treatments (0, 0.01, 10, and 1000 µg/mL $nTiO_2$) into separate
278 statistical groups. The validity of the statistical groups was verified by MANOVA. There are 9
279 distinct statistical groups in the HR dendrogram (Figure 5j, Roman numerals). Although in some
280 cases there are individuals from the same treatment within different clusters, the majority of the
281 clusters were based on the same treatment and there was clear separation of the endpoints related
282 to the exposure concentration.
283
284 3.4. Differences among treatments concerning SR
285 The mortality rate was between 12.3 [6.8]% and 7.8 [4.8]% (mean [SD]) in the $nTiO_2$-
286 exposed embryo-larva and controls, respectively. There was a significant variation among
287 treatments concerning SR at 58 hpe (Figure 5d), 82 hpe (Figure 5e), 106 hpe (Figure 5f), 130–
288 154 hpe (Figure 5g), 178 hpe (Figure 5h), and 202 hpe (Figure 5i). Cluster analysis of SR
289 (Figure 5k) categorized the four $nTiO_2$ treatments into 8 statistically distinct groups in the
290 dendrogram (Figure 5k Roman numerals). We were unable to determine a LC50 for $nTiO_2$.
291
292 3.5. Relationship between HR and SR
293 The SR at 106, 130–154, 178, and 202 hpe was significantly correlated (Figure 5 m-p) to
294 HR at 106 hpe (the time to hatch of all live embryos [total hatching]). But there was no
295 significant relationship between SR and HR at 34 (the day of onset of hatching only in 1000
296 µg/mL $nTiO_2$-exposed embryo groups), 58 (the day of onset of hatching in 0, 0.01, and 10
297 µg/mL $nTiO_2$-exposed embryo groups), and 82 (time to 60% hatch) hpe.

298

299 3.6. $nTiO_2$-induced morphological responses

300 We detected a concentration-dependent precipitation of $nTiO_2$ on embryos within 34 h of
301 exposure (Figure 2, panels a-h) and $nTiO_2$ precipitation on larvae at 58 hpe (Figure 2, panels m-
302 r). Embryos exposed to $nTiO_2$ showed an accelerated (premature) hatching Figure 5 (a). We also
303 observed that early hatched embryos had a significantly (ANOVA; $p<0.001$) smaller size (mean
304 [SD] = 2.12 [0.24] mm) and larger yolk sac relative to body size (i.e. a lower TBL to BD-II ratio;
305 mean [SD] = 2.83 [0.40]) at 34 hpe (Figure 2, panels i-l) compared to control (mean [SD] = 2.87
306 [0.11] mm and mean [SD] = 4.28[0.29], respectively) (Figure 2, at 58 hpe: panel m). Some of the
307 $nTiO_2$-exposed animals (mean [SD] = 8.0 [3.1]%) also had a bent trunk at 58 hpe (Figure 2,
308 panels n, p-r).

309 Figure 2 illustrates a concentration-dependent depletion of the yolk sac at 82 (panels s-v)
310 and 106 hpe (panels w-z) and $nTiO_2$ precipitation on larvae at 82 (panel v), 106 (panel z), and
311 130 hpe (panel ad). A clear morphological difference among $nTiO_2$ treatment groups was not
312 found at 130, 154, 178, and 202 hpe.

313

314 3.7. Variation among treatments concerning MCs

315 The $nTiO_2$-exposed groups significantly differed from controls for the changes in MCs at
316 82 hpe (for BL-82, PoPB-82, BL/APB-82, BL/BD2-82, BL/HL-82, APB/PoPB-82, PoPB/BD1-
317 82, and PoPB/BD2-82 [Table 1, rows 13-14, 16, 18-20, 22-23]). Significant differences were
318 also seen at 106 hpe (for APB-106, BD1-106, BD2-106, BL/PoPB-106, BL/BD1-106, BL/BD2-
319 106, APB/PoPB-106, PoPB/BD1-106, PoPB/BD2-106, and BD1/HL-106 [Table 1, rows 25-27,
320 29-31, 33, 36-38]), 130 hpe (for APB/BD1-130 [Table 1, row 41]), 178 hpe (for PoPB-178,

BL/BD2-178, PoPB/BD2-178, and BD1/BD2-178 [Table 1, rows 50-51, 54-54]), and 202 hpe (for BL-202, PoPB-202, BL/BD1-202, BL/BD2-202, PoPB/BD1-202, and PoPB/BD2-202 [Table 1, rows 55-60]).

Embryo-larva exposed to 0.01, 10, and 1000 μg/mL significantly differed from each other based on 9 MCs (BD1 at 106 hpe [denoted as BD1-106], BD2-106, BL/APB-106, APB/HL-106, APB-154, HL-154, APB/BD1-178, BD1/HL-202, and BD2/HL-202 [Table 1, rows 26-28, 35, 42-43, 52, 61-62]), 9 (BD2-106, BL/APB-106, BL/HL-106, APB-130, HL-130, APB/BD1-154, BL-178, APB-178, and BD1/BD2-178 [Table 1, rows 27-28, 32, 39-40, 45, 48-49, 54]), and 13 (for BD1-82, BL/PoPB-82, BL/BD2-82, APB/BD1-82, PoPB/BD1-82, PoPB/HL-82, BD2-106, BL/PoPB-106, APB/PoPB-106, APB/BD2-106, BL/BD2-154, PoPB/BD2-154, and BD1/BD2-154 [Table 1, rows 15, 17-18, 21-22, 24, 27, 29, 33-34, 44, 46-47]), respectively.

Cluster analysis was performed on MCs (Figure 5l) that categorized the four $nTiO_2$ treatments into separate statistical groups, to create a dendrogram that allows visual examination of the distribution of the four treatment groups. There was a significant separation based on the concentration of $nTiO_2$. There were 9 (Figure 5l, the Roman numerals) distinct groups in the dendrograms. Although in some cases there are individuals from the same treatment group within different clusters, the majority of the clusters were based on the same treatment and there was clear separation of the endpoints that were related to the exposure concentration.

3.8. Relationship of MCs with HR and SR

The MCs (as dependent variables) significantly (either negatively [boldface] or positively) correlated to HR (as the independent variable) at 58 (Table 2, rows 1-17), 82 (Table 2, rows 18-25), and 106 (Table 2, rows 26-32) hpe by 32 simple regression models. SR and its

344 standard deviation (SRSD) (Table 3) at 106 (row 1), 130 (rows 2-12), 178 (rows 13-29), and 202
345 (rows 30-55) hpe were significantly negatively (Table 3, boldface) or positively correlated to
346 MCs (or their ratios) at 82 (Table 3, rows 1, 2, 4, 5, 13, 20, 21, 34, 35, 36-41), 106 (Table 2, rows
347 3, 14, 42-46), 130 (Table 3, rows 6-12, 22-28), 154 (Table 3, rows 30, 47-51), 178 (Table 3, rows
348 15-19, 29, 31-33, 52, and 53), and 220 (Table 3, rows 54 and 55) hpe by 55 simple regression
349 models.
350
351 **4. Discussion**
352 Embryo-larvae viability parameters (such as "hatching events" and "survivability" at
353 different embryo/larvae stages) are important endpoints that have been used as criteria (1) to
354 characterize $nTiO_2$-induced general responses in zebrafish (Yeo and Jo,2007; Xu et al. 2012;
355 Kovrižnych et al., 2013; Wang et al., 2014), (2) to evaluate the effects of exposure to $nTiO_2$ on
356 survivability in a disease outbreak (Jovanovic et al., 2015), (3) to characterize toxicity of
357 different $nTiO_2$ formulations (Clemente et al., 2014), (4) to assess effect of light on $nTiO_2$
358 toxicity (Ma et al., 2013; Clemente et al., 2014), (5) to survey $nTiO_2$ toxicity combined with
359 other chemicals (Yan et al.,2014), (6) to discriminate the toxicity of different forms of $nTiO_2$
360 (ion, particle, and bulk) (Vicario-Parés et al., 2014), and (7) to follow $nTiO_2$ toxicity in offspring
361 (Fouqueray et al., 2013). Embryo-larvae phenotypic characteristics are other most common
362 endpoints that are considered to characterize $nTiO_2$ toxicity in zebrafish embryo-larvae.
363 In the studies mentioned in the previous paragraph embryo-larvae viability parameters
364 such as "hatchability" and "survivability" (in most studies at a single embryonic/larval stage) and
365 phenotypic responses were considered as independent endpoints to characterize $nTiO_2$-induced
366 toxicity. None of the studies evaluated relationships either among viability parameters (e.g.

between hatching events and survivability) or between viability parameters and other endpoints (e.g. between phenotypic alterations and hatching events or survivability). The experimental design of the above mentioned studies did not enable them to explore such relationships. Evaluation of such relationships needs more endpoints, i.e. a big data set while prior studies used limited endpoints to address their hypotheses. In the earlier studies the phenotypic analyses of $nTiO_2$-induced defects was performed based upon morphological characteristics. Generating quantitative data from morphometric characteristics (MC) has been largely ignored or under-used.

In the current study "hatchability", "survivability", and 21 morphometric characteristics (each at multiple times, both during $nTiO_2$ exposure and a depuration period) were determined to characterize $nTiO_2$-induced toxicity in zebrafish embryo-larvae. In fact, 171 sub-lethal (i.e. hatchability at 3 times and 21 morphometric characteristics at 8 time points) and survivability at 8 times were used to address the hypotheses of this study. The values of the 179 endpoints provided with enough data to define relationships between sub-lethal endpoints (e.g. between hatching events and morphometric alterations) and between sub-lethal and acute endpoints (e.g. between survivability and hatching event or morphometric alterations). To our knowledge the current study is the first in which morphometric alterations have comprehensively been considered to characterize $nTiO_2$-induced toxicity.

4.1. Ti^{+4} concentration

In the current study, Ti^{+4} accounted for less than 0.00001% of the total titanium content in the $nTiO_2$. This is consistent with reports where the titanium was cited as a low concentration element in aquatic ecosystems (Orians et al. 1990; Croot 2011), artificial solutions (Kumazawa

et al. 2002; Yamamoto et al. 2004; Zhu et al. 2008; Johnston et al. 2010; Vicario-Parés et al. 2014; He et al. 2014), and in the aqueous environment of cells (Kumazawa et al. 2002).

4.2. Comparison of Ti^{+4}-treated groups with control

There were no significant differences between Ti^{+4}-treated groups and controls concerning HR, SR, and MC, i.e. 0.0001 µg/mL Ti^{+4} did not have any effect on embryo-larvae morphometrics and viability (Table 1). This is hypothesized to be attributed to the fact that 0.0001 µg/mL is a relatively low exposure concentration of Ti^{+4} (Monteith et al. 1993; Liao et al. 1999; Cadosch et al. 2009).

4.3. $nTiO_2$-induced variation in SR and HR

Statistical analyses based on SR descriptive statistics at 58, 82-154, 178, and 202 hpe revealed significant variability among $nTiO_2$-exposed and unexposed embryo-larvae, even at environmentally-relevant concentrations (0.01 µg/mL [Mueller and Nowack 2008]) but also among the $nTiO_2$-exposed groups. The findings contradict some early studies in which zebrafish embryo-larvae (Zhu et al. 2008; Xu et al. 2012; Kovrižnych et al. 2013; Vicario-Parés et al. 2014), medaka (Paterson et al. 2011), and fathead minnow (Jovanović et al. 2011a) have been cited as low sensitive models to $nTiO_2$ acute toxicity.

By day 4 (106 hpe), all individuals had hatched. There was no statistically significant difference between treatment groups concerning HR (Figure 5c). This is contrary to the study of Yan et al. (2014) in which the exposure of embryos to 40 mg/L of $nTiO_2$ led to a significantly decreased HR compared to lower concentrations and controls. The different biological responses to $nTiO_2$ exposure observed among studies might be attributed to characteristics of the

nanoparticles (size [Lovern and Klaper 2006], crystal form [Zhu et al. 2009], morphology, chemical composition [Wiesner et al. 2006]), dispersant (e.g., pH [Pettibone et al. 2008; French et al. 2009], ionic strength [Truong et al. 2012]), as well as the exposure protocol (e.g. duration of exposure [Federici et al. 2007]).

Hatching began on day 2 (34 hpe). Early hatching (2% at 34 hpe) was only observed in 1000 µg/mL $nTiO_2$-exposed embryos. There was a significant concentration-dependent HR difference among $nTiO_2$-exposed and unexposed groups at 58 hpe (Figure 5a). At 82 hpe > 50% of embryos hatched (Figure 5b) with a concentration-dependent difference among the four treatment groups. The data show a concentration-dependent acceleration in hatching in $nTiO_2$-exposed treatment groups (0.01, 10, and 1000 µg/mL) compared to control.

$nTiO_2$-induced changes in hatching time have also been observed in other studies, e.g. in the studies of Kovrižnych et al. (2013), Ma and Diamond (2013), Fouqueray et al. (2013), and Samaee et al. (2015) the effects of $nTiO_2$ on hatching time were reported as accelerated (premature) hatching while in the study of Xu et al. (2012), the effects were reported as delayed hatching.

The above results show a lack of significant difference among treatment groups concerning total hatching while there was significantly variability concerning hatching time. This illustrates that the hatching time is a more sensitive endpoint to characterize $nTiO_2$-induced responses compared to total hatching, consistent with Barton (2002) who suggested the change in hatching time as an important stress response of fish larvae.

4.4. Relationship of SR with hatching events

435 Many available nanomaterials (e.g. $nTiO_2$) do not exhibit a difference in LC50 values
436 between the egg and larvae stage (Kovrižnych et al. 2013), or cause lethal effects unless the
437 concentrations are grossly exaggerated. Thus, the possibility to evaluate hatching events such as
438 hatching time and calculate a concentration that can induce premature or delayed hatching is
439 important (Kovrižnych et al. 2013). Despite the reported effects of $nTiO_2$ on hatching time both
440 in the current study and earlier studies (Xu et al. 2012; Kovrižnych et al. 2013, Ma and Diamond
441 2013, Fouqueray et al. 2013, and Samaee et al. 2015), the relationship of the $nTiO_2$-induced
442 change in hatching time and total hatching to embryo-larvae development and survivability in
443 zebrafish has yet to be determined.
444 As an attempt to address the question in this study, SR at different larval stages (106,
445 130, 154, 178, and 202 hpe) was found to be significantly correlated to HR at 106 hpe (time to
446 hatch of all live embryos [or total HR]) while the SR was not correlated to the $nTiO_2$-induced
447 change in hatching time (HR at 58 [the day of onset of hatching in all treatment groups] and 82
448 [time to 60% hatch]) hpe. This means that although the magnitude of total hatching can
449 significantly affect embryo-larvae survivability, the $nTiO_2$-induced change in hatching time does
450 not directly affect the survivability.
451
452 4.5. $nTiO_2$-induced morphological variation among treatments
453 We detected a concentration-dependent $nTiO_2$ precipitation on the embryos within 34 h
454 of exposure (Figure 2, panels a-h), consistent with Bai et al. (2010), Paterson et al. (2011), and
455 Yan et al. (2014). When the concentration of $nTiO_2$ was increased to 1000 µg/mL the egg
456 envelope surface became turbid and difficult to observe (Figure 2, panel g and h). Embryos
457 exposed to $nTiO_2$ showed accelerated hatching (Figure 2 panels g-l), compared to controls

458 (panels a-b) at 34 hpe. For changes in hatching time see Paterson et al. (2011) and references
459 therein.

460 We observed that early hatched embryos had a significantly smaller size (mean [SD] =
461 2.12 [0.24] mm) and larger yolk sac relative to body size (a lower TBL to BD-II ratio; mean
462 [SD] = 2.83 [0.40]) (Figure 2, panels i-l) compared to control (mean [SD] = 2.87 [0.11] mm and
463 mean [SD] = 4.28 [0.29], respectively) (Figure 2, panel m). This has been reported for medaka
464 (Leung and Bulkley 1979; Paterson et al 2011) and in an earlier study on zebrafish (Samaee et al.
465 2015) following $nTiO_2$ exposure. Such phenotypic alterations have already been discussed by
466 Samaee et al. (2015).

467 Other observations included bent trunk larvae at 58 hpe (Figure 2, panels 1, n, p-r) and
468 the presence of $nTiO_2$ precipitation on larvae at 58 (Figure 2, panels n-r), 82, 106, and 130 hpe
469 (Figure 2, panels v,z,ad). The bent trunk was the only $nTiO_2$-induced abnormality observed in
470 the current study, consistent with Yan et al. (2014) who reported no significant morphological
471 abnormality in zebrafish embryos exposed to $nTiO_2$ suspensions of different concentrations. In
472 earlier studies other types of $nTiO_2$-induced morphological abnormalities have been reported
473 (Yeo and Kang 2009; Yeo and Kim 2010; He et al. 2014; Wang et al. 2014; Yan et al. 2014).
474 The variations in $nTiO_2$-induced morphological responses observed in different studies can be
475 attributed to the characteristics of the nanoparticles (Lovern and Klaper 2006; Zhu et al. 2009;
476 Wiesner et al. 2006), dispersant (Pettibone et al. 2008; French et al. 2009; Truong et al. 2012), as
477 well as exposure protocol (Federici et al. 2007).

478 The lack of clear morphological differences among $nTiO_2$ treatments at 130, 154, 178,
479 and 202 hpe (Figure 2) shows that the morphological changes observed at early larval stages, 34,
480 58, 82, and 106 hpe (Figure 2) disappear at advanced developmental stages. Therefore, the

morphological changes observed in the current study could not be considered as potential endpoints (markers) to predict zebrafish embryo-larvae success (survivability).

4.6. $nTiO_2$-induced morphometric variation among treatments

A cluster analysis placed the four $nTiO_2$ treatment groups into separated statistical groups (Figure 5l). The analysis revealed that there was significant morphometric variation between $nTiO_2$-exposed and unexposed groups, but also among the exposed groups. These morphometric variabilities reveal the potential of the MCs to characterize $nTiO_2$-induced responses of embryo-larvae even at environmentally-relevant concentrations (0.01 μg/mL; Mueller and Nowack 2008).

4.7. Relationship of MCs with HR and SR

In the current study morphometric alterations were found to be stable through all zebrafish larval stages, therefore contrary to morphological changes, those that disappeared at advanced larval stages can be nominated as potential endpoints to predict larval success. To evaluate this potential, simple regression models were formulated between MCs and SR. Based on the regression models, MCs significantly correlated to HR, SR, or both. Regarding the significant associations, three groups of MCs were characterized:

The first group of MCs (Tables 2 and 3, non-underlined data) significantly correlated (either positively or negatively [boldface]) to HR (at 58, 82, and 106 hpe) and SR (during $nTiO_2$ exposure [106 and 130 hpe] and during depuration [178 and 202 hpe). The relationship of these MCs with HR at 58, 82, and 106 hpe shows that the morphometric variations are a consequence of the $nTiO_2$-induced changes in hatching time. The synchronous association of the MCs with

504 both HR and SR indicates an indirect effect of the $nTiO_2$-induced change in hatching time on
505 survivability.

506 The second group of MCs significantly correlated to hatchability at 58, 82, and 106 hpe
507 (Table 2, underlined data) but was not significantly associated with SR. This means that the
508 morphometric alterations induced by the change in hatching time do not affect embryo-larvae
509 SR.

510 The third group of MCs was correlated to SR but not HR (during $nTiO_2$ exposure [106
511 and 130 hpe] and during depuration [178 and 202 hpe [Table 3, underlined data]). This shows
512 that the alteration in this group of MCs cannot be attributed to the $nTiO_2$-induced changes in
513 hatching time. Probably they have appeared either during exposure of developing larvae to $nTiO_2$
514 (SR at 106 and 130 hpe) or during depuration (SR at 178 and 202 hpe).

515 On one hand the presented relationships in the three above paragraphs show that two
516 groups of MCs (group 1 [Tables 2 and 3, non-underlined data] and group 3 [Table 3, underlined
517 data]) are significantly correlated to SR. The significant associations of the two groups of MCs
518 with SR clearly highlight the potential of morphometric alterations (as sublethal endpoints) to
519 predict survivability (as an acute endpoint). On the other hand the synchronous correlation of the
520 group 1 MCs [Tables 2 and 2, non-underlined data] with both HR and SR demonstrates the
521 significant effect of the $nTiO_2$-induced change in hatching time on embryo-larvae survivability
522 (as the one of objectives of the study).

523 In general, a key element complicating the establishment of a link between exposure and
524 a health defect is the time that elapses between exposure and outward response or development
525 of the health defect (Gluckman et al. 2008; Barouki et al. 2012). Thus, it may take years for an
526 individual to present a health defect and in addition may pass on these adverse health effects to

527 future generations (Jirtle and Skinner 2007). In zebrafish the morphometric alterations appeared
528 within a short period of exposure to different concentrations of $nTiO_2$ (even at environmentally-
529 relevant concentrations) and could predict later-in-life consequences of an embryonic exposure
530 to $nTiO_2$. Therefore zebrafish can be considered as a potential biological predictor of the acute
531 toxicity of nTiO2. This is contrary to studies in which the embryo-larvae of zebrafish (Zhu et al.
532 2008; Xu et al. 2012; Kovrižnych et al. 2013), medaka (Paterson et al. 2011), and fathead
533 minnow (Jovanović et al. 2011a) have been cited as low sensitive models to $nTiO_2$ acute toxicity
534 based solely on the failure to generate LC50 at environmentally-relevant concentrations.
535
536 4.8. Conclusions
537 1) In the current study, univariate and multivariate analyses that included HR and SR, as
538 well as MC values differentiated $nTiO_2$-induced responses (even at environmentally-relevant
539 concentrations) of zebrafish embryo-larvae. 2) Exposure of embryos to $nTiO_2$ led to a significant
540 concentration-dependent change in hatching time (an $nTiO_2$-accelerated [premature] hatching),
541 consistent with previous studies. 3) Total hatching (HR at 106 hpe) was significantly correlated
542 to SR but there was not a significant relationship between the change in hatching time (HR at 34,
543 58 and 82 hpe) and SR. This suggests that the $nTiO_2$-induced change in hatching time does not
544 directly affect embryo-larvae survivability. 4) Larval morphometric alterations were significantly
545 correlated to both $nTiO_2$-induced change in hatching time and total hatching, suggesting that
546 $nTiO_2$-induced changes in hatching events can affect embryo-larvae development. 5) Most of the
547 evaluated morphometric variations were significantly correlated to both the change in hatching
548 time and SR. This clearly provides evidence of the indirect effect of the $nTiO_2$-induced change in
549 hatching time on embryo-larvae survivability in zebrafish. 6) The MCs whose variations are

550 correlated to embryo-larvae SR can be considered as potential endpoints to predict embryo-
551 larvae survivability in an $nTiO_2$-toxicity test. 7) The above mentioned findings provide evidence
552 of the significant influence of the hatching events, i.e. $nTiO_2$-induced change in hatching time
553 and total hatching, on zebrafish embryo-larvae development and survivability. 8) The results
554 suggest zebrafish can be considered as a potential biological predictor of the acute toxicity of
555 $nTiO_2$.
556
557 Acknowledgments
558 The authors are grateful to Prof. Dr. Christopher Joseph Martyniuk (Center for
559 Environmental and Human Toxicology, University of Florida, USA) for his helpful scientific and
560 linguistic comments during preparation of the current manuscript.
561
562 **References**
563 Adams L, Lyon D, Alvarez P. 2006. Comparative eco-toxicity of nanoscale TiO_2, SiO_2, and ZnO
564 water suspensions. *Water Res* 40:3527–32.
565 Bai W, Zhang Z, Tian W, He X, Ma Y, Zhao Y, Chai Z. 2010. Toxicity of zinc oxide
566 nanoparticles to zebrafish embryo: a physicochemical study of toxicity mechanism. *J*
567 *Nanopart Res* 12:1645–1654.
568 Bar-Ilan O, Albrecht RM, Fako VE, Furgeson DY. 2009. Toxicity assessments of multisized
569 gold and silver nanoparticles in zebrafish embryos. Small 5(16):1897–910.
570 Barouki R, Gluckman PD, Grandjean P, Hanson M, Heindel JJ. 2012. Developmental origins of
571 non-communicable disease: implications for research and public health. *Environ Health*
572 11:1–9.

573 Barton BA. 2002. Stress in fishes: A diversity of responses with particular reference to changes
574 in circulating corticosteroids. *Integr Comp Biol* 42:517–525.
575 Braunbeck T, Böttcher M, Hollert H, Kosmehl T, Lammer E, Leist E, Rudolf M, Seitz N. 2005.
576 Towards an alternative for the acute fish LC50 test in chemical assessment: the fish
577 embryo toxicity test goes multi-species—an update. *ALTEX* 22:87–102.
578 Braunbeck T, Lammer E. 2006. Background paper on fish embryo toxicity assays. Germany,
579 Federal Environment Agency (UBA contract number 203 85 422), pp 1–298.
580 Cadosch D, Chan E, Gautschi OP, Filgueira L. 2009. Metal is not inert: Role of metal ions
581 released by biocorrosion in aseptic loosening—Current concepts. *J Biomed Mater Res A*
582 91:1252–1262.
583 Chen TH, Lin CY, Tseng MC. 2011. Behavioral effects of titanium dioxide nanoparticles on
584 larval zebrafish (*Danio rerio*). *Mar Pollut Bull* 63(5-12):303–8.
585 Clemente Z, Castro VL, Moura MA, Jonsson CM, Fraceto LF. 2014. Toxicity assessment of
586 TiO_2 nanoparticles in zebrafish embryos under different exposure conditions. *Aquat*
587 *Toxicol* 147:129–39.
588 Colvin VL. 2003. The potential environmental impact of engineered nanomaterials. *Nature*
589 *Biotechnol* 21:1166–1170.
590 Croot PL. 2011. Rapid determination of picomolar titanium in seawater with catalytic cathodic
591 stripping voltammetry. *Anal Chem* 83:6395–6400.
592 Dalai S, Pakrashi S, Kumar RSS, Chandrasekaran N, Mukherjee A. 2012. A comparative
593 cytotoxicity study of TiO_2 nanoparticles under light and dark conditions at low exposure
594 concentrations. *Toxicol Res* 1:116–130.

595 Evonik Industries. 2007. Product Information Sheet, Aeroxide® TiO_2 P-25 Hydrophilic Fumed
596 Titanium Dioxide. USA, NJ, Parsippany.
597 Faria M, Navas JM, Soares AMVM, Barata C. 2014. Oxidative stress effects of titanium dioxide
598 nanoparticle aggregates in zebrafish embryos. Sci Total Environ 470–471:379–389.
599 Federici G, Shaw BJ, Handy RD 2007. Toxicity of titanium dioxide nanoparticles to rainbow
600 trout (*Oncorhynchus mykiss*): gill injury, oxidative stress, and other physiological effects.
601 *Aquat Tox* 84:415–430.
602 Fouqueray M, Noury P, Dherret L, Chaurand P, Abbaci K, Labille J, Rose J, Garric J. 2013.
603 Exposure of juvenile *Danio rerio* to aged TiO_2 nanomaterial from sunscreen. *Environ Sci*
604 *Pollut Res Int* 20(5):3340–50.
605 French RA, Jacobsen AR, Kim B, Isley SL, Penn RL, Baveye PC. 2009. Influence of ionic
606 strength, pH, and cation valence on aggregation kinetics of titanium dioxide
607 nanoparticles. *Environ Sci Technol* 43:1354–1359.
608 Gluckman PD, Hanson MA, Cooper C, Thornburg KL. 2008. Effect of in utero and early-life
609 conditions on adult health and disease. *N Engl J Med* 359:61–73.
610 Goolish EM, Okutake K. 1999. Lack of gas bladder inflation by the larvae of zebrafish in the
611 absence of an air–water interface. *J Fish Biol* 55:1054–1063.
612 Griffitt RJ, Hyndman K, Denslow ND, Barber DS. 2009. Comparison of molecular and
613 histological changes in zebrafish gills exposed to metallic nanoparticles. *Toxicol Sci*
614 107(2):404–415.
615 Hall S, Bradley T, Moore JT, Kuykindall T, Minella L. 2009. Acute and chronic toxicity of
616 nano-scale TiO_2 particles to freshwater fish, cladocerans, and green algae, and effects of
617 organic and inorganic substrate on TiO_2 toxicity. *Nanotoxicology* 3:91–97.

He X, Aker WG, Hwang HM. 2014. An in vivo study on the photo-enhanced toxicities of S-doped TiO_2 nanoparticles to zebrafish embryos (*Danio rerio*) in terms of malformation, mortality, rheotaxis dysfunction, and DNA damage. Nanotoxicology Suppl 1:185–95.

Holmberg A, Schwerte T, Pelster B, Holmgren S. 2004. Ontogeny of the gut motility control system in zebrafish *Danio rerio* embryos and larvae. *J Exp Biol* 207:4085–4094.

Jardine D, Litvak MK. 2003. Direct yolk sac volume manipulation of zebrafish embryos and the relationship between offspring size and yolk sac volume. *J Fish Biol* 63:388–397.

Jirtle RL, Skinner MK. 2007. Environmental epigenomics and disease susceptibility. *Nat Rev Genet* 8:253–262.

Johnston BD, Scown TM, Moger J, Cumberland SA, Baalousha M, Linge K, van Aerle R, Jarvis K, Lead JR, Tyler CR. 2010. Bioavailability of nanoscale metal oxides, TiO_2, CeO_2, and ZnO to fish. Environ Sci Technol 44:1144–1151.

Jovanović B, Anastasova L, Rowe EW, Zhang Y, Clapp AR, Palić D. 2011a. Effects of nanosized titanium dioxide on innate immune system of fathead minnow (*Pimephales promelas* Rafinesque, 1820). *Ecotox Environ Safe* 74:675–683.

Jovanović B, Ji T, Palić D. 2011b. Gene expression of zebrafish embryos exposed to titanium dioxide nanoparticles and hydroxylated fullerenes. Ecotoxicol Environ Saf 74:1518–1525.

Jovanović B, Whitley EM, Kimura K, Crumpton A, Palić D. 2015. Titanium dioxide nanoparticles enhance mortality of fish exposed to bacterial pathogens. *Environ Pollut* 203:153–164.

639 Kim, M.-S, Louis KM, Pedersen JA, Hamers RJ, Petersonad RE, Heideman W. 2014. Using
640 citrate-functionalized TiO_2 nanoparticles to study the effect of particle size on zebrafish
641 embryo toxicity. Analyst 139:964–972.
642 Kovrižnych JA, Sotníková R, Zeljenková D, Rollerová E, Szabová E, Wimmerová S. 2013.
643 Acute toxicity of 31 different nanoparticles to zebrafish (*Danio rerio*) tested in adulthood
644 and in early life stages – comparative study. *Interdiscip Toxicol* 6(2):67–73.
645 Kumazawa R, Watari F, Takashi N, Tanimura Y, Uo M, Totsuka Y. 2002. Effects of Ti ions and
646 particles on neutrophil function and morphology. *Biomaterials* 23:3757–3764.
647 Lammer E, Carr GJ, Wendler K, Rawlings JM, Belanger SE, Braunbeck T. 2009. Is the fish
648 embryo toxicity test (FET) with the zebrafish (*Danio rerio*) a potential alternative for the
649 fish acute toxicity test? *Comp Biochem Physiol C* 149:196–209.
650 Lawrence C. 2007. The husbandry of zebrafish (*Danio rerio*): a review. Aquaculture 269:1–20.
651 León A, Reuquen P, Garín C, Segura R, Vargas P, Zapata P, Orihuela PA. 2017. FTIR and
652 Raman characterization of TiO_2 nanoparticles coated with polyethylene glycol as carrier
653 for 2-methoxyestradiol. *Appl Sci* 7:49.
654 Leung T.-y, Bulkley R. 1979. Effects of petroleum hydrocarbons on length of incubation and
655 hatching success in the Japanese Medaka. *Bull Environ Contam Toxicol* 23:236–243.
656 Li Y, Zhang W, Niu J, Chen Y. 2013. Surface-coating-dependent dissolution, aggregation, and
657 reactive oxygen species (ROS) generation of silver nanoparticles under different
658 irradiation conditions. *Environ Sci Technol* 47:10293−10301.
659 Liao H, Wurtz T, Li J. 1999. Influence of titanium ion on mineral formation and properties of
660 osteoid nodules in rat calvaria cultures. *J Biomed Mater Res* 47:220–227.

661 Liu R, Lin S, Rallo R, Zhao Y, Damoiseaux R, Xia T, Lin S, Nel A, Cohen Y. 2012. Automated
662 phenotype recognition for zebrafish embryo based in vivo high throughput toxicity
663 screening of engineered nano-materials. *PLoS ONE* 7(4):e35014.
664 Lovern SB, Klaper R. 2006. Daphnia magna mortality when exposed to titanium dioxide and
665 fullerene (C60) nanoparticles. *Environ Toxicol Chem* 25:1132–1137.
666 Ma H, Diamond S. 2013. Phototoxicity of TiO_2 nanoparticles to zebrafish (*Danio rerio*) is
667 dependent on life stage. *Environ Toxicol Chemi* 32(9):2139–2143.
668 Menard A, Drobne D, Jemec A. 2011. Ecotoxicity of nanosized TiO_2. Review of *in vivo* data.
669 *Environ Pollut* 159:677e684.
670 Metcalfe C, Bennett E, Chappell M, Steevens J, Depledge M, Goss G, Goudey G, Kaczmar S,
671 O'Brien N, Picado A, Ramadan AB. 2009. SMARTEN: strategic management and
672 assessment of risks and toxicity of engineered nanomaterials. In: Linkov I, Steevens J,
673 eds, Nanomaterials: Risks and Benefits. NATO Science for Security and Peace Series –
674 C: Environmental Security. The Netherlands, Dordrecht, Springer, pp 95–109.
675 Monteith MR, Zaharias R, Keller JC. 1993. Effect of soluble Ti on in vitro osteoblast
676 mineralization. *J Dent Res* 73:400.
677 Moore MN. 2006. Do nanoparticles present ecotoxicological risks for the health of the aquatic
678 environment? *Environ Int* 32:967–976.
679 Mueller NC, Nowack B. 2008. Exposure modeling of engineered nanoparticles in the
680 environment. Environ Sci Technol 42:4447–4453.
681 Mugundan S, Rajamannan G, Viruthagiri N, Shanmugam R, Gobi P. 2015. Synthesis and
682 characterization of undoped and cobalt-doped TiO_2 nanoparticles via sol-gel technique.
683 *Appl Nanosci* 5:449–456.

684 Nadica D, Abazovic M, Comor M, Dramicanin D, Jovanovic S, Jovan M. 2006.
685 Photoluminescence of anatase and rutile TiO_2 particles. *J Phys Chem B* 110:25366–
686 25370.
687 Ohno T, Sarukawa K, Tokeida K, Matsumura M. 2001. Morphology of a TiO_2 photocatalyst
688 (Degussa, P-25) consisting of anatase and rutile crystalline phases. *J Catal* 203:82–86.
689 Oliver, AL.-S, Muñoz-Olivas R, Landaluze JS, Rainieri S, Cámara C. 2015. Bioaccumulation of
690 ionic titanium and titanium dioxide nanoparticles in zebrafish eleutheroembryos.
691 Nanotoxicology 9(7):835–42.
692 Orians KJ, Boyle EA, Bruland KW. 1990. Dissolved titanium in the open ocean. *Nature*
693 348:322–325.
694 Paterson G, Ataria JM, Hoque ME, Burns DC, Metcalfe CD. 2011. The toxicity of titanium
695 dioxide nanopowder to early life stages of the Japanese medaka (*Oryzias latipes*).
696 Chemosphere 82:1002–1009.
697 Pettibone JM, Cwiertny DM, Scherer M, Grassian VH. 2008. Adsorption of organic acids on
698 TiO2 nanoparticles: Effects of pH, nanoparticle size, and nanoparticle aggregation.
699 *Langmuir* 24:6659–6667.
700 Rasmussen, K., et al. 2014. Titanium Dioxide, NM-100, NM-101, NM-102, NM-103, NM-104,
701 NM-105: characterization and physico-chemical properties. European Commission.
702 Luxembourg: Publications Office of the European Union. ISBN 978-92-79-38188-1, pp
703 218.
704 Samaee S.-M, Rabbani S, Jovanović B, Mohajeri-Tehrani MR, Haghpanah V. 2015. Efficacy of
705 the hatching event in assessing the embryo toxicity of the nano-sized TiO_2 particles in

zebrafish: A comparison between two different classes of hatching-derived variables. *Ecotox Environ Safe* 116:121–128.

Service RF. 2004. Nanotechnology grows up. Science 304:1732–1734.

Truong L, Zaikova T, Richman EK, Hutchison JE, Tanguay RL. 2012. Media ionic strength impacts embryonic responses to engineered nanoparticle exposure. *Nanotoxicology* 6:691–699.

Varga ZM. 2011. Aquaculture and husbandry at the Zebrafish International Resource Center. *Method Cell Biol* 104:453–78.

Vicario-Parés U, Castañaga L, Lacave JM, Oron M, Reip P, Berhanu D, Valsami-Jones E, Cajaraville MP, Orbea A. 2014. Comparative toxicity of metal oxide nanoparticles (CuO, ZnO, and TiO_2) to developing zebrafish embryos. J Nanopart Res 16:2550.

Vogt A, Cholewinski A, Shen X, Nelson SG, Lazo JS, Tsang M, Hukriede NA. 2009. Automated image-based phenotypic analysis in zebrafish embryos. *Dev Dyn* 238(3):656–663.

Wang YJ, He ZZ, Fang YW, Xu Y, Chen YN, Wang GQ, Yang YQ, Yang Z, Li YH. 2014. Effect of titanium dioxide nanoparticles on zebrafish embryos and developing retina. *Int J Ophthalmol* 7(6):917–23.

Westerfield M. 2000. The Zebrafish book: A guide for the laboratory use of zebrafish (*Danio rerio*). USA, Eugene, University of Oregon Press.

Wiesner MR, Lowry GV, Alvarez P, Dionysiou D, Biswas P. 2006. Assessing the risks of manufactured nanomaterials. *Environ Sci* 40:4336–4345.

Wilson C. 2012. Aspects of larval rearing. *ILAR J* 53(2):169–178.

727 Xu Z, Zhang Y.-L, Song C, Wu L.-L, Gao H.-W. 2012. Interactions of Hydroxyapatite with
728 proteins and its toxicological effect to zebrafish embryos development. *PLoS ONE*
729 7(4):e32818.
730 Yamamoto A, Honma R, Sumita M, Hanawa T. 2004. Cytotoxicity evaluation of ceramic
731 particles of different sizes and shapes. *J Biomed Mater Res* 68A:244–256.
732 Yan J, Lin B, Hu C, Zhang H, Lin Z, Xi Z. 2014. The combined toxicological effects of titanium
733 dioxide nanoparticles and bisphenol A on zebrafish embryos. *Nanoscale Res Lett* 9:406.
734 Yeo M.-K, Jo YH. 2007. Bio-toxicity of titanium dioxide nano particles (P-25) in zebrafish
735 development stage. *J Environ Toxicol* 22(3):189–196.
736 Yeo M.-K, Kang M. 2009. Effects of CuxTiOy nanometer particles on biological toxicity during
737 zebrafish embryogenesis. *Korean J Chem Eng* 26:711–718.
738 Yeo M.-K, Kim H.-E. 2010. Gene expression in zebrafish embryos following exposure to TiO_2
739 nanoparticles. *Mol Cell Toxicol* 6:97–104.
740 Zhu RR, Wang SL, Chao J, Shi DL, Zhang R, Sun XY, Yao SD. 2009. Bio-effects of Nano-TiO_2
741 on DNA and cellular ultrastructure with different polymorph and size. *Mater Sci Eng C*
742 29:691–696.
743 Zhu XS, Zhu L, Duan Z, Qi R, Li Y, Lang YJ. 2008. Comparative toxicity of several metal oxide
744 nano-particle aqueous suspensions to zebrafish (*Danio rerio*) early developmental stage.
745 *Environ Sci Health A* 43:278–284.
746
747
748
749

TABLES

TABLE 1: Comparison of treatment groups (0, Ti^{+4}, 0.01, 10, and 1000 μg/mL) concerning magnitude of TiO_2-induced changes in morphometric characteristics.

Footnote: Data are mean [SD]. Values superscripted with the same letter are not significantly different, $p < 0.05$. See the legend of Figure 3 for abbreviations of the morphometric characteristics (MCs).

TABLE 2: Simple regression equations, correlation (r^2), F and p values of the significant relationships found between the hatching rate (HR; at 58, 82, and 106 hpe) and the morphometric characteristics (MC; at 82, 106, 130, 154, 178, and 202 hpe).

771 **Footnote:** The non-underlined, underlined, and boldface data show MCs that are correlated to
772 both HR and SR, are only correlated to HR, and are negatively correlated to HR and/or SR,
773 respectively. See figure 3 legend for MC abbreviations.
774
775 **TABLE 3:** Simple regression equations, explanatory effect (r^2), F and p values of the significant
776 relationships between the mean and standard deviation (SRSD) of survival rate (SR at 106, 130,
777 178, and 202 hpe) and morphometric characteristics (MC at 82, 106, 130, 154, 178, and 202
778 hpe).
779 **Footnote:** The non-underlined, underlined, and boldface data show MCs that are correlated to
780 both HR and SR, are only correlated to SR, and are negatively correlated to HR and/or SR,
781 respectively. See figure 3 legend for MC abbreviations.
782
783
784 **FIGURES**
785 **FIGURE 1:** The zebrafish embryo-larvae observation time points.
786
787 **FIGURE 2:** Photomicrographs of zebrafish embryo-larvae. Images are zebrafish embryo-larvae
788 at 34, 58, 82, 106, 130, 154, 178, and 202 hpe exposed to 0 (control), 0.01, 10, and 1000 µg/mL
789 $nTiO_2$. Scale bar, 1 mm.
790
791 **FIGURE 3:** Morphometric characteristics determined in zebrafish embryo-larvae. The
792 landmarks on the zebra fish larvae schematics depict the characteristics that were utilized for
793 screening $nTiO_2$-induced responses. TBL (total body length): greatest horizontal body distance

794 — anterior-most part of head to the end of body. APB (anterior part of body): anterior-most part
795 of head to the posterior-most insertion of yolk sac. PoPB (posterior part of body): the posterior-
796 most insertion of yolk sac to the end of body. HL (head length): anterior-most part of head to the
797 place where the head is connected to the body. BD-I (body depth I): vertical distance from
798 posterior-most insertion of yolk sac to upper surface of body. BD-II (body depth II): greatest
799 vertical body distance. Fifteen ratios were calculated from the six morphometric characteristics
800 TBL/APB, TBL/PoPB, TBL/BD-I, TBL/BD-II, TBL/HL, APB/PoPB, APB/BD-I, APB/BD-I,
801 APB/HL, PoPB/BD-I, PoPB/BD-II, PoPB/HL, BD-I/BD-II, BD-I/HL, and BD-II/HL.
802
803 **FIGURE 4:** Physicochemical characteristics of $nTiO_2$ particles. (a,f) TEM micrographs for
804 $nTiO_2$ nanoparticles dispersed in test solution (egg water) immediately after suspension
805 preparation (a) and after 24 h (f). (b-e, g-j) $nTiO_2$ particle size at times representing exposure
806 conditions immediately after suspension preparation (b-d), and 24 h later (g-i). (e, j) Z-potentials
807 of $nTiO_2$ in egg water. ATR-FTIR spectra for $nTiO_2$ immediately after preparation of suspension
808 (k), and after 12 (l) and 24 h (m).
809
810 **FIGURE 5:** Variation among treatment groups concerning hatching rate (HR) (a-c), survival rate
811 (SR) (d-i),. (a-c) The dendrograms (j-l) illustrate significant differences among zebrafish
812 embryo-larvae exposed to 0, 0.01, 10, and 1000 μg/mL $nTiO_2$ for HR (j), SR (k), and MCs (l).
813 The Roman numerals show the number of created groups by cluster analysis. Scatter plots show
814 significant relationships between SR at different developmental stages (as dependent variables)
815 and HR at 106 hpe (as the independent variable) (m-p).

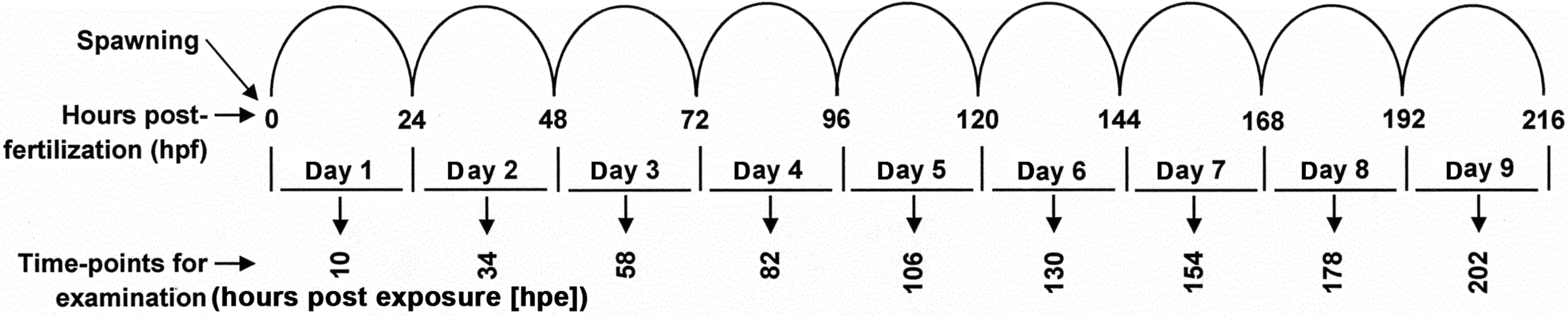
Spawning
Hours post-fertilization (hpf)
0
24
48
72
96
120
144
168
192
216
Day 1
Day 2
Day 3
Day 4
Day 5
Day 6
Day 7
Day 8
Day 9
Time-points for examination (hours post exposure [hpe])
10
34
58
82
106
130
154
178
202

34 hpe

58 hpe

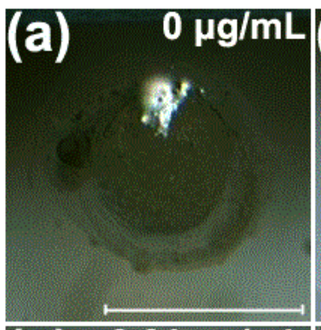

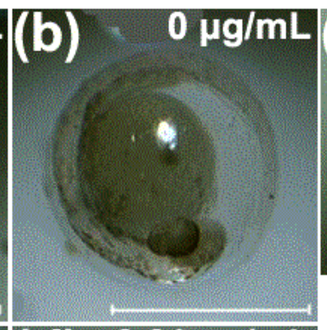

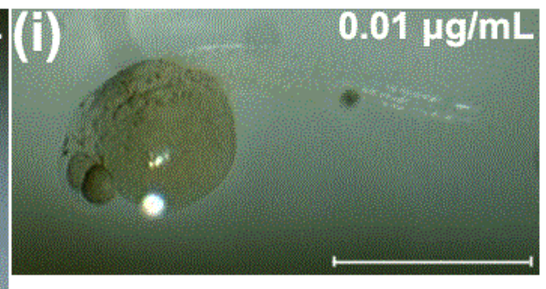

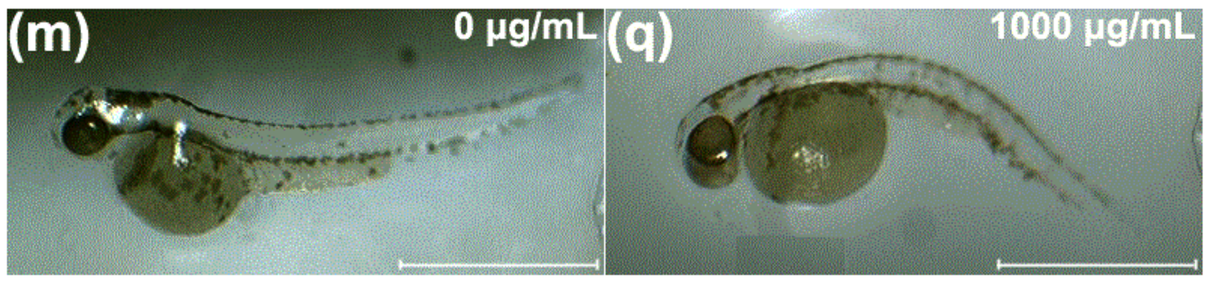

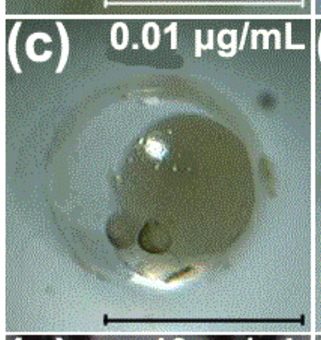

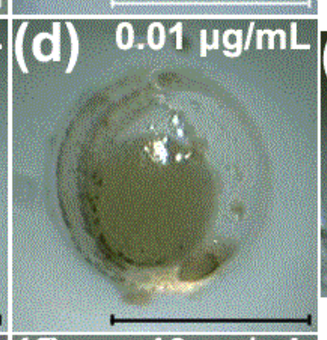

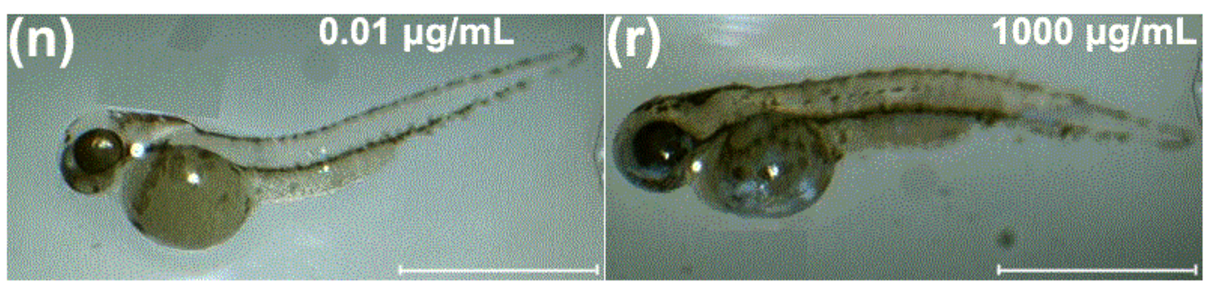

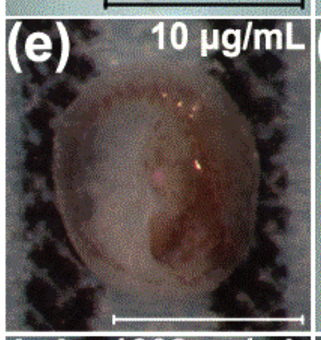

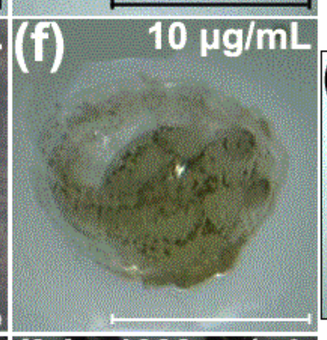

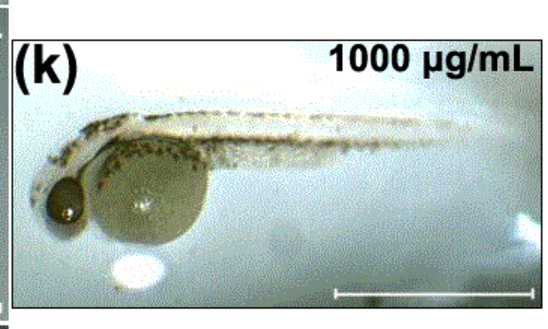

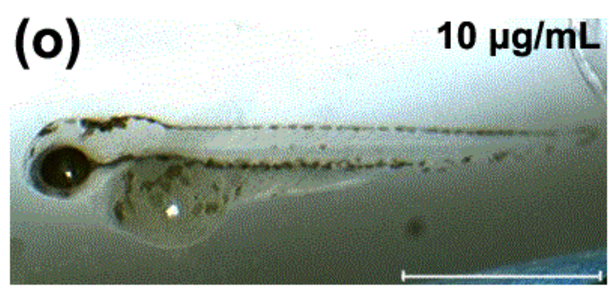

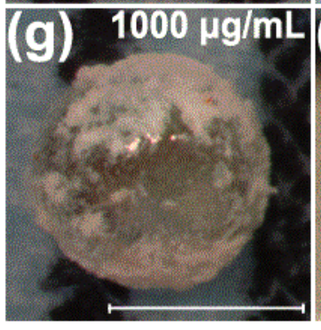

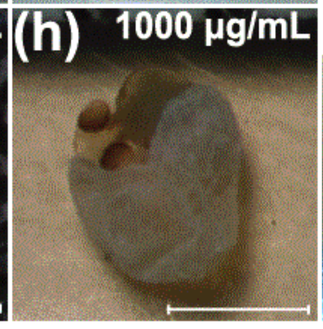

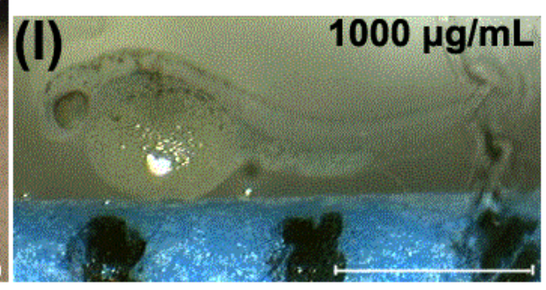

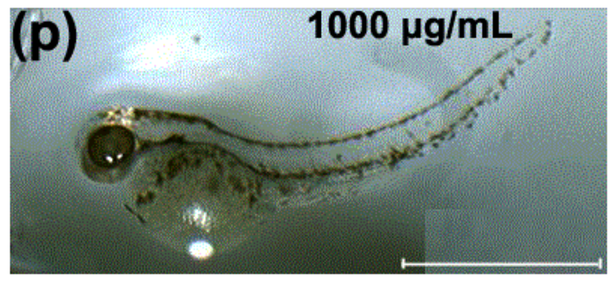

82 hpe

106 hpe

130 hpe

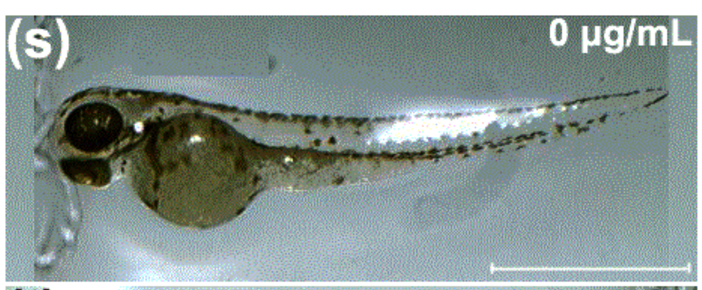

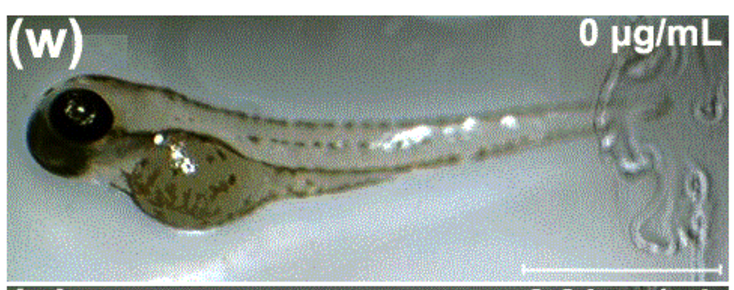

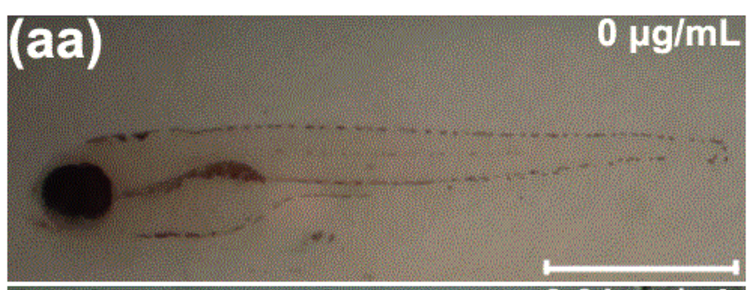

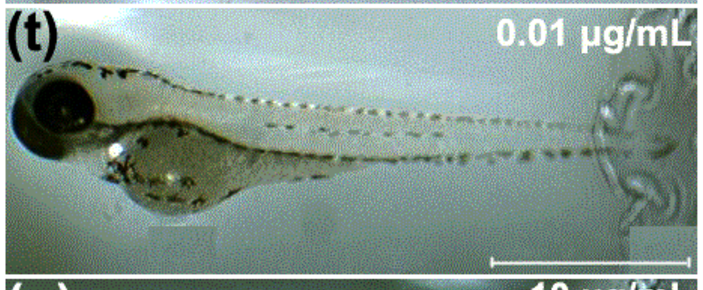

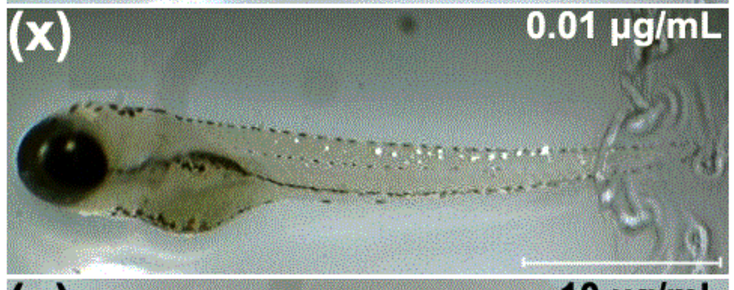

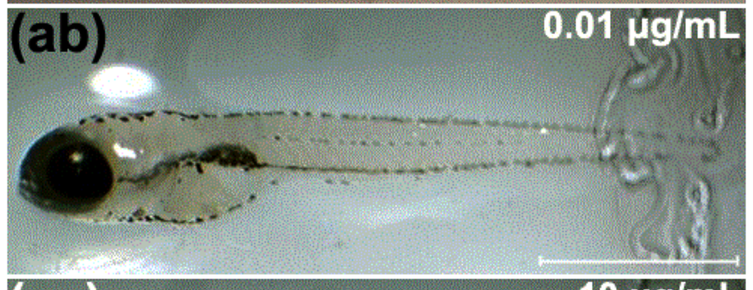

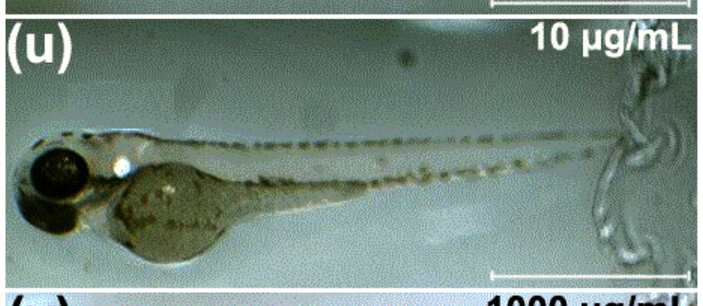

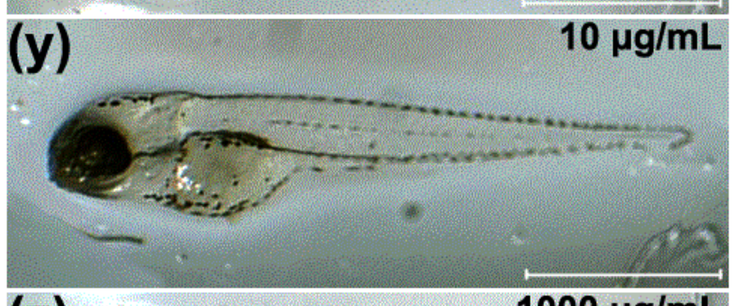

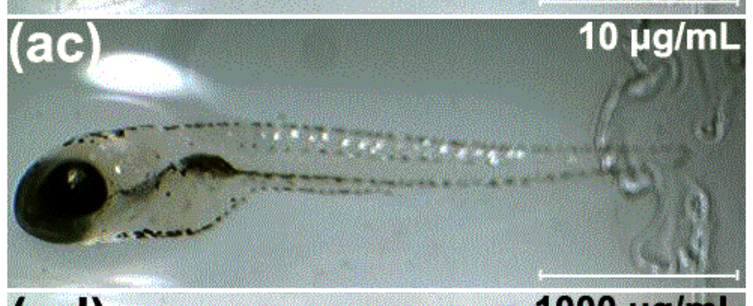

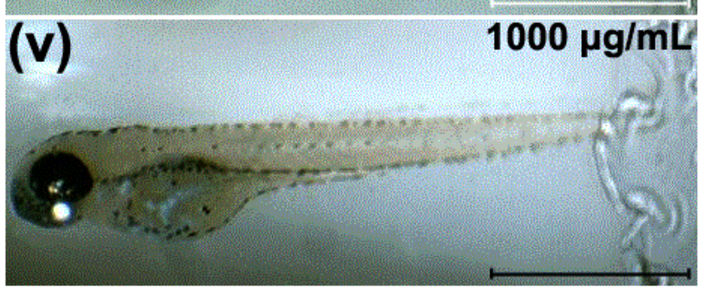

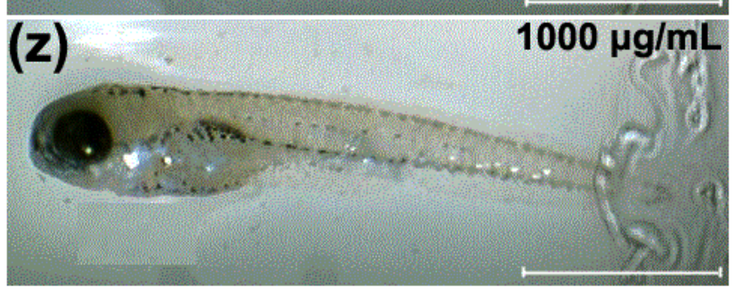

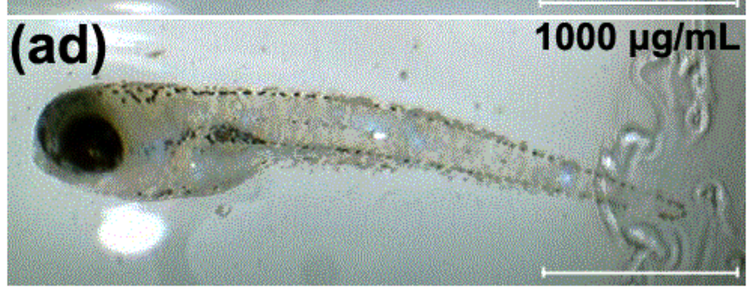

154 hpe

178 hpe

202 hpe

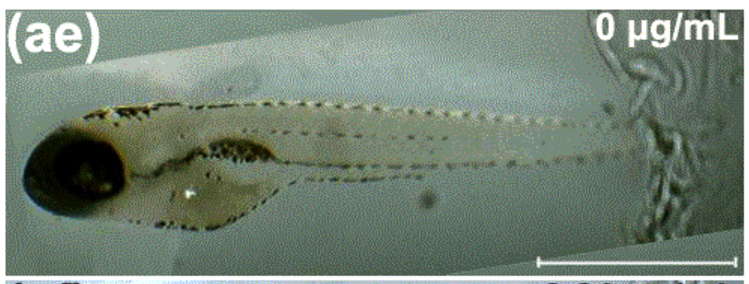

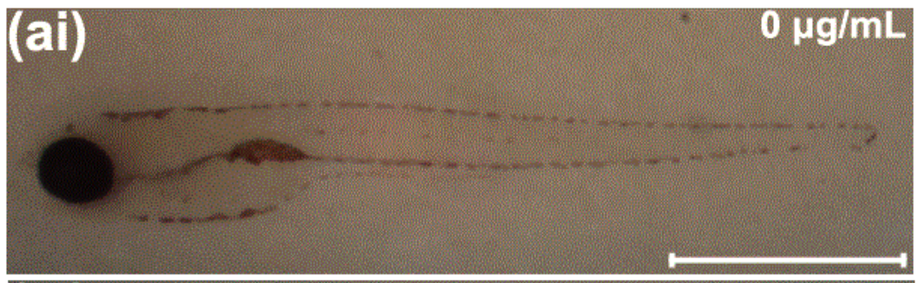

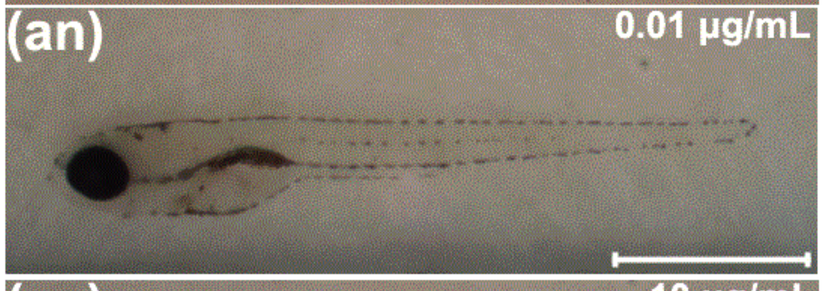

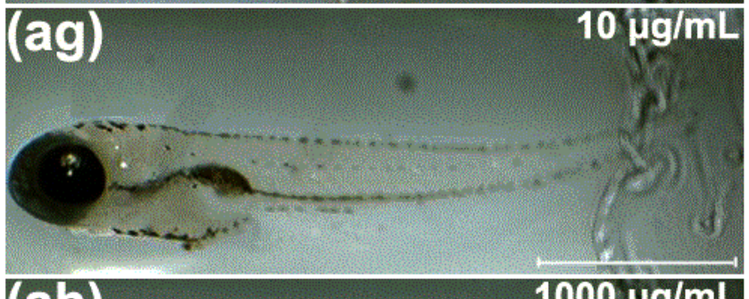

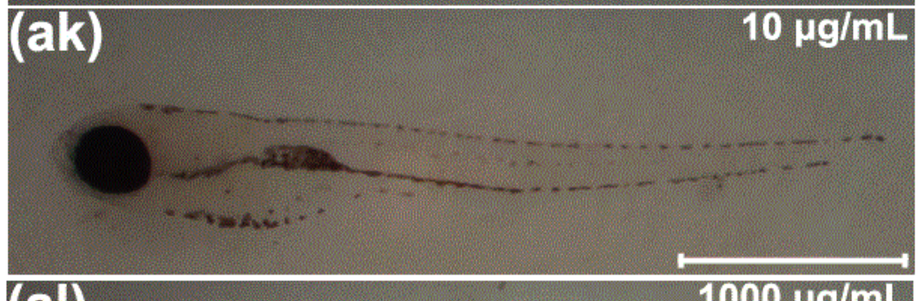

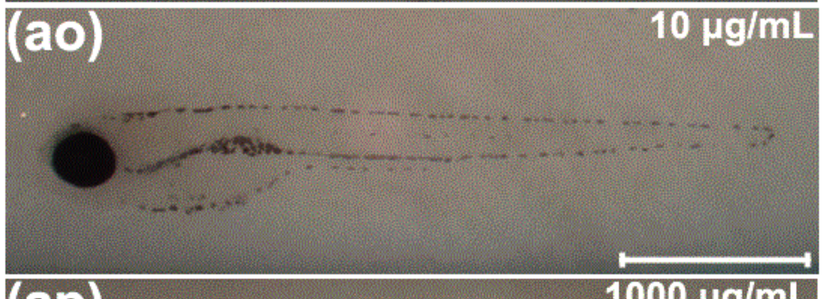

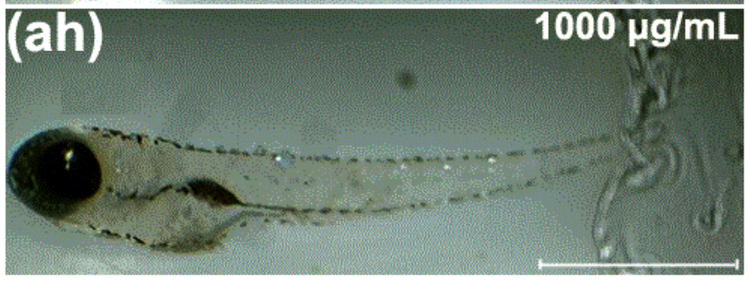

(a)

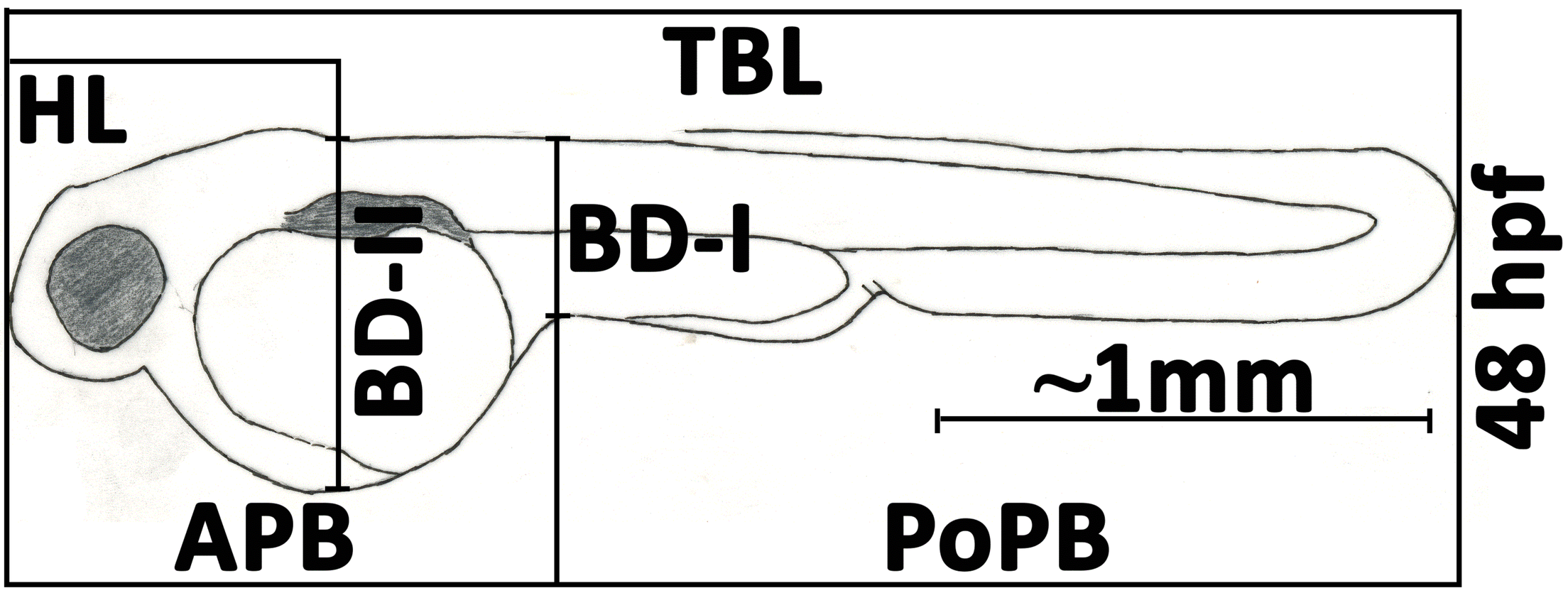
TBL
HL
BD-II
BD-I
~1mm
48 hpf
APB
PoPB

(b)

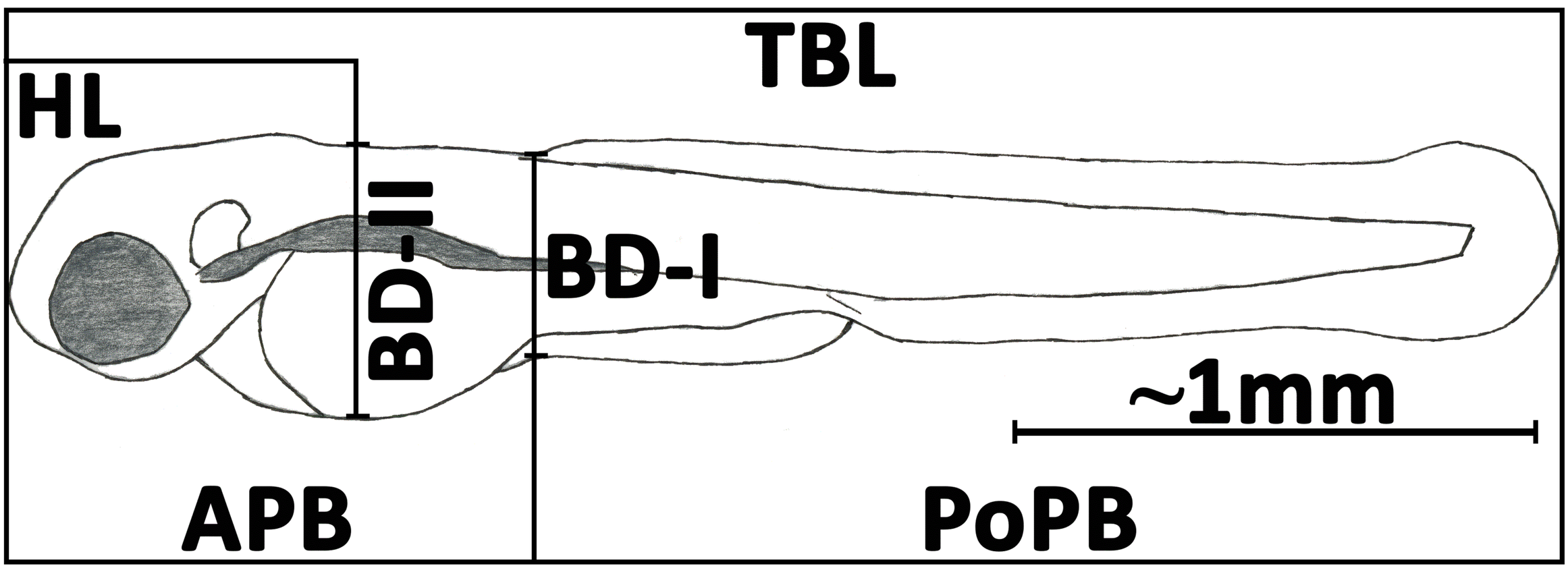
TBL
HL
BD-II
BD-I
~1mm
72 hpf
APB
PoPB

(c)

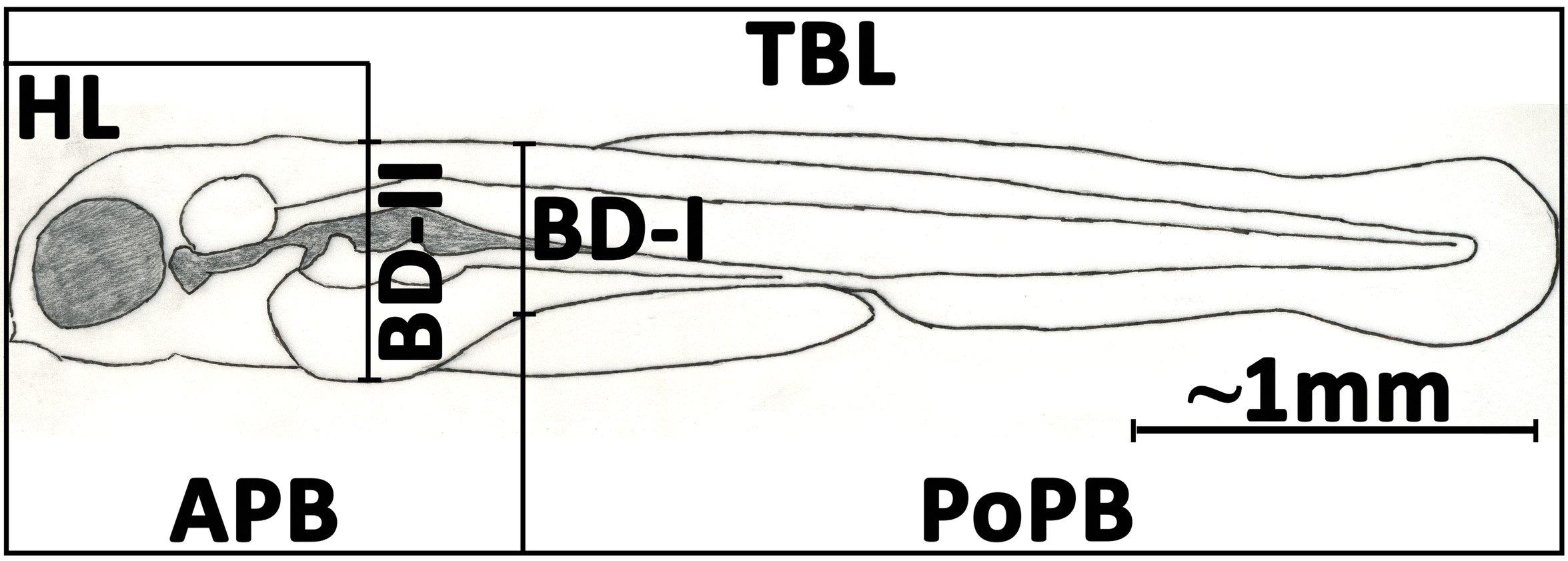
TBL
HL
BD-II
BD-I
~1mm
96 hpf
APB
PoPB

(d)

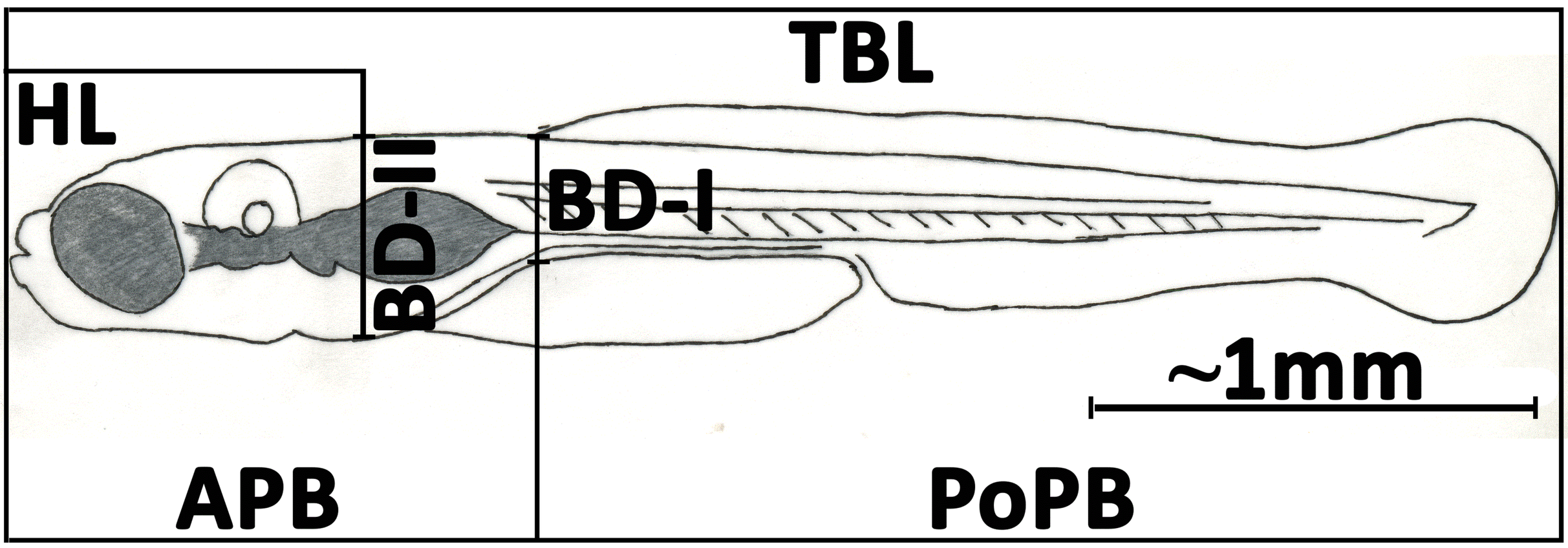
TBL
HL
BD-II
BD-I
~1mm
120 hpf
APB
PoPB

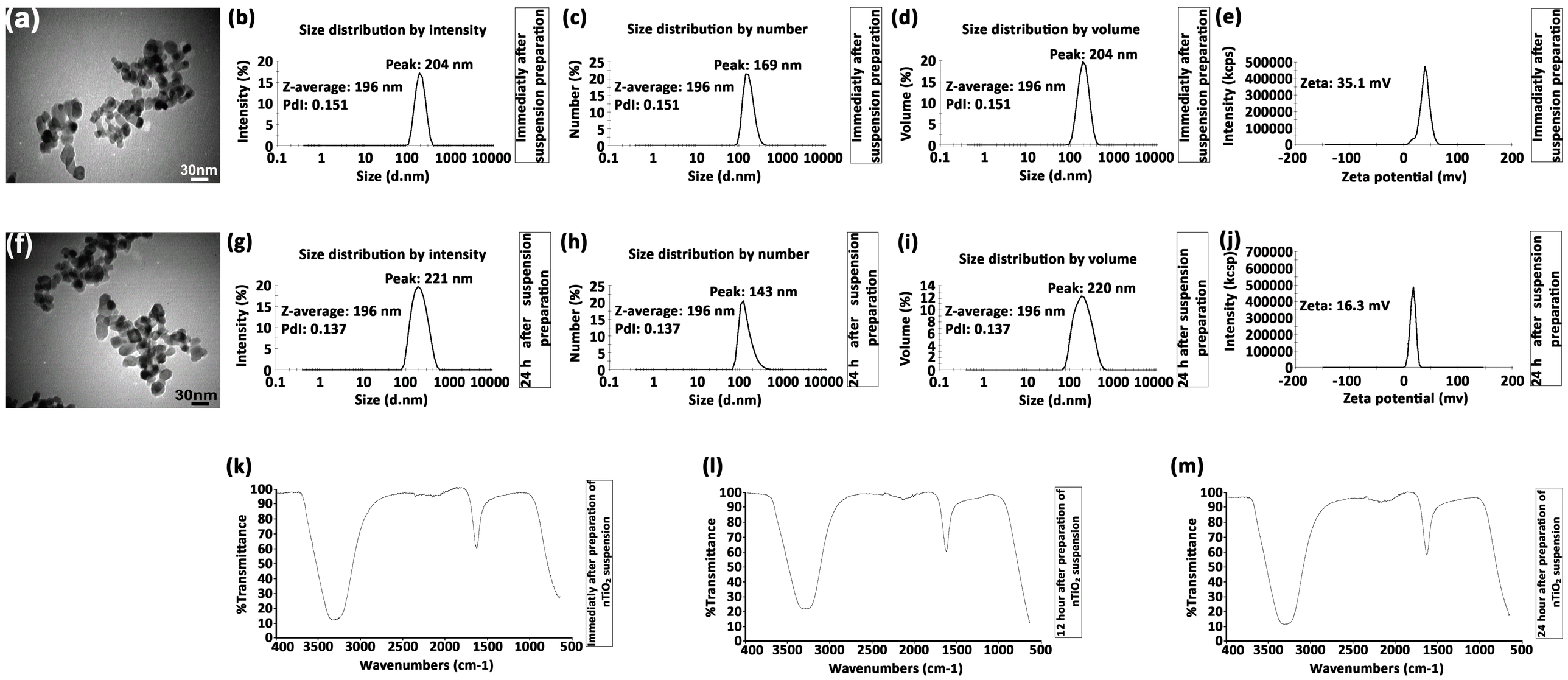
(a)
30nm
(b)
Size distribution by intensity
Peak: 204 nm
Z-average: 196 nm
PdI: 0.151
Intensity (%)
Size (d.nm)
Immediatly after suspension preparation
(c)
Size distribution by number
Peak: 169 nm
Z-average: 196 nm
PdI: 0.151
Number (%)
Size (d.nm)
Immediatly after suspension preparation
(d)
Size distribution by volume
Peak: 204 nm
Z-average: 196 nm
PdI: 0.151
Volume (%)
Size (d.nm)
Immediatly after suspension preparation
(e)
Zeta: 35.1 mV
Intensity (kcps)
Zeta potential (mv)
Immadiatly after suspension preparation
(f)
30nm
(g)
Size distribution by intensity
Peak: 221 nm
Z-average: 196 nm
PdI: 0.137
Intensity (%)
Size (d.nm)
24 h after suspension preparation
(h)
Size distribution by number
Peak: 143 nm
Z-average: 196 nm
PdI: 0.137
Number (%)
Size (d.nm)
24 h after suspension preparation
(i)
Size distribution by volume
Peak: 220 nm
Z-average: 196 nm
PdI: 0.137
Volume (%)
Size (d.nm)
24 h after suspension preparation
(j)
Zeta: 16.3 mV
Intensity (kcsp)
Zeta potential (mv)
24 h after suspension preparation
(k)
%Transmittance
Wavenumbers (cm-1)
Immediatly after preparation of nTiO2 suspension
(l)
%Transmittance
Wavenumbers (cm-1)
12 hour after preparation of nTiO2 suspension
(m)
%Transmittance
Wavenumbers (cm-1)
24 hour after preparation of nTiO2 suspension

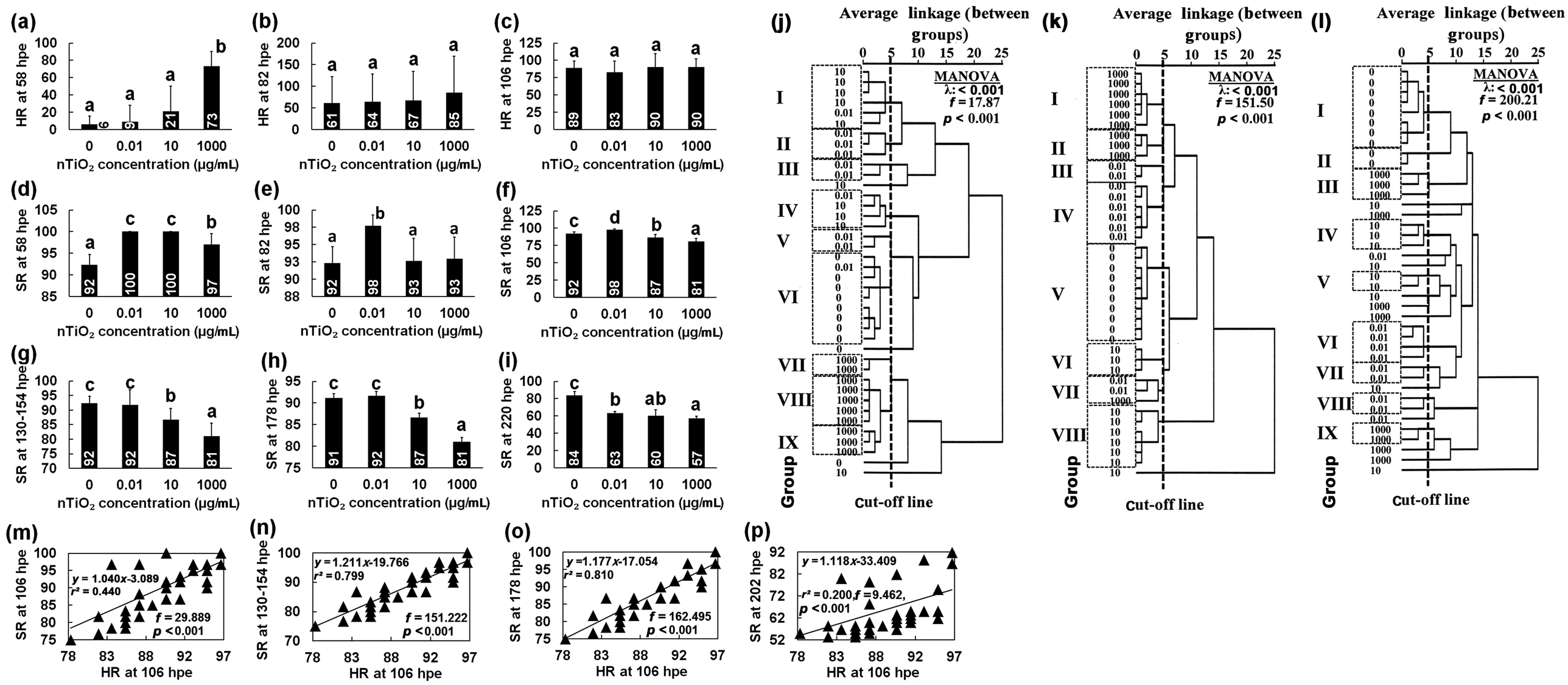
(a)
HR at 58 hpe
nTiO2 concentration (μg/mL)
(b)
HR at 82 hpe
nTiO2 concentration (μg/mL)
(c)
HR at 106 hpe
nTiO2 concentration (μg/mL)
(d)
SR at 58 hpe
nTiO2 concentration (μg/mL)
(e)
SR at 82 hpe
nTiO2 concentration (μg/mL)
(f)
SR at 106 hpe
nTiO2 concentration (μg/mL)
(g)
SR at 130-154 hpe
nTiO2 concentration (μg/mL)
(h)
SR at 178 hpe
nTiO2 concentration (μg/mL)
(i)
SR at 220 hpe
nTiO2 concentration (μg/mL)
(j)
Average linkage (between groups)
MANOVA
λ: < 0.001
f = 17.87
p < 0.001
Group
Cut-off line
(k)
Average linkage (between groups)
MANOVA
λ: < 0.001
f = 151.50
p < 0.001
Group
Cut-off line
(l)
Average linkage (between groups)
MANOVA
λ: < 0.001
f = 200.21
p < 0.001
Group
Cut-off line
(m)
SR at 106 hpe
y = 1.040x-3.089
r² = 0.440
f = 29.889
p < 0.001
HR at 106 hpe
(n)
SR at 130-154 hpe
y = 1.211x-19.766
r² = 0.799
f = 151.222
p < 0.001
HR at 106 hpe
(o)
SR at 178 hpe
y = 1.177x-17.054
r² = 0.810
f = 162.495
p < 0.001
HR at 106 hpe
(p)
SR at 202 hpe
y = 1.118x-33.409
r² = 0.200, f = 9.462,
p < 0.001
HR at 106 hpe

Table 1.

No.	Variables	Ti^{4+} and $nTiO_2$ exposure concentration (μg/mL)				
		0 (n=100)	**Ti^{4+}: 0.0001** (n=100)	**0.01** (n=100)	**10** (n=100)	**1000** (n=100)
1	HR-34	0.00 [0.00]$^{(a)}$	0.00[0.00]$^{(a)}$	0.00[0.00]$^{(a)}$	0.00[0.00]$^{(a)}$	2.00[6.30]$^{(b)}$
2	HR-58	6.00 [9.70]$^{(a)}$	1.43[3.78]$^{(a)}$	9.00[19.10]$^{(a)}$	21.00[29.20]$^{(b)}$	73.00[17.00]$^{(c)}$
3	HR-82	61.00 [29.20]$^{(a)}$	63.33[19.66]$^{(a)}$	64.00[29.10]$^{(a)}$	67.00[37.10]$^{(a)}$	85.00[14.30]$^{(b)}$
4	HR-106	89.00 [9.90]$^{(a)}$	90.00[14.14]$^{(a)}$	83.00[16.40]$^{(a)}$	90.00[19.40]$^{(a)}$	90.00[12.50]$^{(a)}$
5	SR-34	100.00 [0.00]$^{(a)}$	100.00[0.00]$^{(a)}$	100.00[0.00]$^{(a)}$	100.00[0.00]$^{(a)}$	100.00[0.00]$^{(a)}$
6	SR-58	92.34 [2.39]$^{(a)}$	92.86[1.78]$^{(a)}$	100.00[0.00]$^{(c)}$	100.00[0.00]$^{(c)}$	97.00[2.58]$^{(b)}$
7	SR-82	92.34 [2.39]$^{(a)}$	92.86[1.78]$^{(a)}$	97.69[1.59]$^{(b)}$	92.67[3.26]$^{(a)}$	92.99[3.12]$^{(a)}$
8	SR-106	92.34 [2.39]$^{(c)}$	92.86[1.78]$^{(c)}$	97.69[1.59]$^{(d)}$	86.68[3.93]$^{(b)}$	81.01[4.53]$^{(a)}$
9	SR-130	92.34 [2.39]$^{(c)}$	92.86[1.78]$^{(c)}$	91.69[5.27]$^{(c)}$	86.68[3.93]$^{(b)}$	81.01[4.53]$^{(a)}$
10	SR-154	92.34 [2.39]$^{(c)}$	92.86[1.78]$^{(c)}$	91.69[5.27]$^{(c)}$	86.68[3.93]$^{(b)}$	81.01[4.53]$^{(a)}$
11	SR-178	91.18 [2.22]$^{(c)}$	91.86[2.13]$^{(c)}$	91.69[5.27]$^{(c)}$	86.68[3.93]$^{(b)}$	81.01[4.53]$^{(a)}$
12	SR-220	83.50 [4.81]$^{(c)}$	63.00[1.71]$^{(c)}$	63.17[1.82]$^{(b)}$	60.33[6.97]$^{(ab)}$	57.17[2.50]$^{(a)}$
13	BL-82	2.87 [0.22]$^{(a)}$	2.92[0.24]$^{(a)}$	3.30[0.12]$^{(b)}$	3.20[0.14]$^{(b)}$	3.13[0.22]$^{(b)}$
14	PoPB-82	1.74 [0.19]$^{(a)}$	1.78[0.21]$^{(a)}$	2.07[0.09]$^{(b)}$	2.03[0.11]$^{(b)}$	2.21[0.32]$^{(b)}$
15	BD1-82	0.38 [0.00]$^{(b)}$	0.38[0.00]$^{(b)}$	0.40[0.02]$^{(b)}$	0.40[0.01]$^{(b)}$	0.36[0.04]$^{(a)}$
16	BL/APB-82	2.53 [0.13]$^{(a)}$	2.56[0.14]$^{(a)}$	2.69[0.08]$^{(b)}$	2.74[0.07]$^{(b)}$	2.66[0.04]$^{(b)}$
17	BL/PoPB-82	1.66[0.06]$^{(b)}$	1.64[0.05]$^{(b)}$	1.59[0.03]$^{(b)}$	1.58[0.02]$^{(b)}$	1.46[0.19]$^{(a)}$
18	BL/BD2-82	4.25[0.38]$^{(a)}$	4.33[0.42]$^{(a)}$	5.51[0.45]$^{(c)}$	5.48[0.30]$^{(c)}$	4.93[0.94]$^{(b)}$
19	BL/HL-82	3.95[0.05]$^{(a)}$	3.97[0.06]$^{(a)}$	4.14[0.14]$^{(b)}$	4.14[0.14]$^{(b)}$	4.26[0.10]$^{(b)}$
20	APB/PoPB-82	0.66[0.06]$^{(b)}$	0.65[0.06]$^{(b)}$	0.59[0.03]$^{(a)}$	0.58[0.02]$^{(a)}$	0.55[0.07]$^{(a)}$
21	APB/BD1-82	2.95[0.07]$^{(a)}$	2.97[0.07]$^{(a)}$	3.10[0.28]$^{(a)}$	2.92[0.15]$^{(a)}$	3.34[0.24]$^{(b)}$
22	PoPB/BD1-82	4.54[0.48]$^{(a)}$	4.65[0.52]$^{(a)}$	5.22[0.45]$^{(b)}$	5.09[0.40]$^{(b)}$	6.19[0.46]$^{(c)}$
23	PoPB/BD2-82	2.58[0.31]$^{(a)}$	2.65[0.34]$^{(a)}$	3.46[0.30]$^{(b)}$	3.48[0.23]$^{(b)}$	3.46[0.71]$^{(b)}$
24	PoPB/HL-82	2.38[0.11]$^{(a)}$	2.41[0.12]$^{(a)}$	2.60[0.12]$^{(ab)}$	2.69[0.14]$^{(b)}$	3.02[0.47]$^{(c)}$
25	APB-106	1.37[0.08]$^{(b)}$	1.39[0.09]$^{(b)}$	1.26[0.05]$^{(a)}$	1.28[0.06]$^{(a)}$	1.30[0.06]$^{(a)}$
26	BD1-106	0.40[0.01]$^{(c)}$	0.40[0.01]$^{(c)}$	0.38[0.02]$^{(b)}$	0.36[0.01]$^{(a)}$	0.35[0.01]$^{(a)}$
27	BD2-106	0.63[0.00]$^{(d)}$	0.63[0.00]$^{(d)}$	0.60[0.02]$^{(c)}$	0.58[0.01]$^{(b)}$	0.56[0.03]$^{(a)}$
28	BL/APB-106	2.45[0.12]$^{(ab)}$	2.43[0.13]$^{(a)}$	2.70[0.06]$^{(c)}$	2.62[0.04]$^{(c)}$	2.53[0.10]$^{(b)}$
29	BL/PoPB-106	1.70[0.06]$^{(bc)}$	1.71[0.06]$^{(c)}$	1.59[0.02]$^{(a)}$	1.62[0.02]$^{(a)}$	1.66[0.04]$^{(b)}$
30	BL/BD1-106	8.42[0.22]$^{(a)}$	8.46[0.24]$^{(a)}$	8.91[0.80]$^{(b)}$	9.31[0.23]$^{(c)}$	9.28[0.10]$^{(bc)}$
31	BL/BD2-106	5.32[0.02]$^{(a)}$	5.32[0.02]$^{(a)}$	5.64[0.42]$^{(b)}$	5.75[0.27]$^{(bc)}$	5.93[0.33]$^{(c)}$
32	BL/HL-106	3.99[0.08]$^{(a)}$	3.97[0.08]$^{(a)}$	3.96[0.30]$^{(a)}$	4.17[0.1]8$^{(b)}$	3.96[0.12]$^{(a)}$
33	APB/PoPB-106	0.70[0.06]$^{(bc)}$	0.71[0.06]$^{(c)}$	0.59[0.02]$^{(a)}$	0.62[0.02]$^{(a)}$	0.66[0.04]$^{(b)}$
34	APB/BD2-106	2.18[0.12]$^{(a)}$	2.21[0.13]$^{(a)}$	2.08[0.13]$^{(a)}$	2.20[0.13]$^{(a)}$	2.36[0.18]$^{(b)}$
35	APB/HL-106	1.63[0.05]$^{(b)}$	1.64[0.06]$^{(b)}$	1.46[0.09]$^{(a)}$	1.59[0.05]$^{(b)}$	1.57[0.10]$^{(b)}$
36	PoPB/BD1-106	4.95[0.04]$^{(a)}$	4.94[0.05]$^{(a)}$	5.61[0.52]$^{(b)}$	5.75[0.10]$^{(b)}$	5.59[0.11]$^{(b)}$
37	PoPB/BD2-106	3.14[0.10]$^{(a)}$	3.11[0.11]$^{(a)}$	3.56[0.29]$^{(b)}$	3.55[0.15]$^{(b)}$	3.58[0.21]$^{(b)}$
38	BD1/HL-106	0.48[0.02]$^{(a)}$	0.47[0.02]$^{(a)}$	0.45[0.02]$^{(b)}$	0.45[0.03]$^{(b)}$	0.43[0.01]$^{(b)}$
39	APB-130	1.25[0.05]$^{(a)}$	1.27[0.06]$^{(ab)}$	1.31[0.05]$^{(ab)}$	1.39[0.07]$^{(c)}$	1.32[0.08]$^{(b)}$
40	HL-130	0.83[0.03]$^{(a)}$	0.84[0.04]$^{(a)}$	0.84[0.07]$^{(a)}$	0.90[0.03]$^{(b)}$	0.85[0.05]$^{(a)}$
41	APB/BD1-130	3.31[0.18]$^{(a)}$	3.34[0.19]$^{(a)}$	3.58[0.28]$^{(b)}$	3.75[0.14]$^{(b)}$	3.58[0.29]$^{(b)}$
42	APB-154	1.32[0.02]$^{(b)}$	1.32[0.02]$^{(b)}$	1.23[0.08]$^{(a)}$	1.35[0.08]$^{(b)}$	1.31[0.08]$^{(b)}$
43	HL-154	0.89[0.02]$^{(b)}$	0.89[0.03]$^{(b)}$	0.85[0.03]$^{(a)}$	0.88[0.04]$^{(b)}$	0.89[0.02]$^{(b)}$
44	BL/BD2-154	7.12[0.53]$^{(b)}$	7.22[0.58]$^{(b)}$	7.10[0.35]$^{(b)}$	7.09[0.43]$^{(b)}$	6.39[0.47]$^{(a)}$
45	APB/BD1-154	3.94[0.23]$^{(ab)}$	3.98[0.25]$^{(ab)}$	3.83[0.10]$^{(a)}$	4.15[0.37]$^{(b)}$	3.92[0.12]$^{(ab)}$
46	PoPB/BD2-154	4.57[0.40]$^{(b)}$	4.65[0.43]$^{(b)}$	4.64[0.26]$^{(b)}$	4.44[0.39]$^{(b)}$	4.01[0.41]$^{(a)}$
47	BD1/BD2-154	0.65[0.01]$^{(b)}$	0.65[0.01]$^{(b)}$	0.64[0.01]$^{(b)}$	0.64[0.03]$^{(b)}$	0.61[0.04]$^{(a)}$
48	BL-178	3.85[0.12]$^{(b)}$	3.83[0.13]$^{(b)}$	3.73[0.10]$^{(b)}$	3.53[0.31]$^{(a)}$	3.70[0.03]$^{(b)}$
49	APB-178	1.31[0.02]$^{(b)}$	1.31[0.02]$^{(b)}$	1.32[0.05]$^{(b)}$	1.20[0.13]$^{(a)}$	1.28[0.02]$^{(b)}$
50	PoPB-178	2.54[0.10]$^{(c)}$	2.52[0.11]$^{(bc)}$	2.41[0.06]$^{(ab)}$	2.33[0.20]$^{(a)}$	2.42[0.03]$^{(abc)}$
51	BL/BD2-178	7.91[0.09]$^{(b)}$	7.89[0.09]$^{(b)}$	7.47[0.26]$^{(a)}$	7.45[0.15]$^{(a)}$	7.33[0.11]$^{(a)}$
52	APB/BD1-178	4.00[0.03]$^{(a)}$	4.01[0.04]$^{(a)}$	4.17[0.21]$^{(b)}$	3.87[0.26]$^{(a)}$	3.94[0.10]$^{(a)}$
53	PoPB/BD2-178	5.21[0.11]$^{(b)}$	5.19[0.11]$^{(b)}$	4.83[0.17]$^{(a)}$	4.92[0.15]$^{(a)}$	4.79[0.09]$^{(a)}$
54	BD1/BD2-178	0.67[0.00]$^{(c)}$	0.67[0.00]$^{(c)}$	0.64[0.01]$^{(a)}$	0.65[0.02]$^{(b)}$	0.64[0.01]$^{(a)}$
55	BL-202	3.89[0.06]$^{(b)}$	3.88[0.06]$^{(b)}$	3.71[0.10]$^{(a)}$	3.62[0.15]$^{(a)}$	3.64[0.15]$^{(a)}$
56	PoPB-202	2.56[0.05]$^{(b)}$	2.55[0.05]$^{(b)}$	2.43[0.12]$^{(a)}$	2.36[0.12]$^{(a)}$	2.38[0.08]$^{(a)}$
57	BL/BD1-202	12.49[0.15]$^{(b)}$	12.47[0.16]$^{(b)}$	11.63[0.19]$^{(a)}$	11.86[0.64]$^{(a)}$	11.98[0.75]$^{(a)}$
58	BL/BD2-202	7.99[0.14]$^{(b)}$	7.96[0.16]$^{(b)}$	7.42[0.35]$^{(a)}$	7.35[0.29]$^{(a)}$	7.54[0.48]$^{(a)}$
59	PoPB/BD1-202	8.23[0.13]$^{(b)}$	8.21[0.14]$^{(b)}$	7.61[0.29]$^{(a)}$	7.73[0.34]$^{(a)}$	7.85[0.55]$^{(a)}$
60	PoPB/BD2-202	5.26[0.11]$^{(b)}$	5.24[0.12]$^{(b)}$	4.86[0.33]$^{(a)}$	4.79[0.17]$^{(a)}$	4.94[0.34]$^{(a)}$
61	BD1/HL-202	0.37[0.01]$^{(a)}$	0.37[0.01]$^{(a)}$	0.39[0.02]$^{(b)}$	0.36[0.02]$^{(a)}$	0.36[0.02]$^{(a)}$
62	BD2/HL-202	0.58[0.02]$^{(a)}$	0.58[0.02]$^{(a)}$	0.61[0.01]$^{(b)}$	0.58[0.03]$^{(a)}$	0.58[0.04]$^{(a)}$

Table 2. Table 2. Simple regression equations, correlation (r^2), *F* and *p* values of the significant relationships found between the hatching rate (at 58, 82, and 106 h postexposure) and the morphometric characteristics (at 82, 106, 130, 154, 178, and 202 h postexposure)

No.	Variables			r^2	F	*p*
	Independent	Dependent	Equations			
1	HR-58	PoPB-82	y= 0.004x+1.908	0.229	11.288	0.002
2	HR-58	BD1-82	y=-0.001x+0.398	0.298	16.120	0.001
3	HR-58	BL/PoPB-82	y=-0.003x+1.635	0.352	20.652	0.001
4	HR-58	BL/BD1-82	y= 0.013x+7.853	0.232	11.457	0.002
5	HR-58	APB/PoPB-82	y=-0.001x+0.623	0.263	13.568	0.001
6	HR-58	APB/BD1-82	y= 0.005x+2.964	0.267	13.837	0.001
7	HR-58	PoPB/BD1-82	y= 0.019x+4.801	0.536	43.942	0.001
8	HR-58	PoPB/HL-82	y= 0.008x+2.485	0.428	28.456	0.001
9	HR-58	BD1-106	y= 0.000x+0.386	0.390	24.287	0.001
10	HR-58	BD2-106	y=-0.001x+0.613	0.479	34.902	0.001
11	HR-58	BD1/HL-106	y= 0.000x+0.460	0.219	10.626	0.002
12	HR-58	BD2/HL-106	y=-0.001x+0.732	0.233	11.520	0.002
13	HR-58	APB/BD2-106	y= 0.003x+2.131	0.279	14.691	0.001
14	HR-58	BL/BD2-154	y=-0.011x+7.185	0.335	19.183	0.001
15	HR-58	BD1/BD2-154	y= 0.000x+0.647	0.225	11.024	0.002
16	HR-58	PoPB/BD2-154	y=-0.008x+4.622	0.314	17.384	0.001
17	HR-58	BL/BD2-178	y=-0.005x+7.663	0.293	15.727	0.001
18	HR-82	BD1-82	y=-0.001x+0.449	0.200	9.473	0.001
19	HR-82	PoPB/BD1-82	y= 0.033x+3.078	0.328	18.531	<0.001
20	HR-82	PoPB/HL-82	y= 0.014x+1.750	0.280	14.800	<0.001
21	HR-82	BD1-106	y=-0.001x+0.426	0.220	10.715	0.002
22	HR-82	BD2-106	y=-0.001x+0.686	0.290	15.491	<0.001
23	HR-82	BL/BD2-154	y=-0.020x+8.271	0.239	11.965	0.001
24	HR-82	APB/BD2-154	y=-0.006x+2.932	0.289	15.474	<0.001
25	HR-82	BL/BD2-178	y=-0.010x+8.219	0.234	11.617	0.002
26	HR-106	PoPB/HL-130	y= 1.022x+0.019	0.221	10.772	0.002
27	HR-106	APB/BD1-178	y=-0.022x+5.986	0.250	12.689	0.001
28	HR-106	BD1/BD2-178	y= 0.466x+0.002	0.266	13.792	0.001
29	HR-106	BL/BD1-202	y= 0.065x+6.171	0.258	13.202	0.001
30	HR-106	BL/BD2-202	y= 0.048x+3.350	0.274	14.315	0.001
31	HR-106	PoPB/BD1-202	y= 0.051x+3.354	0.298	16.124	<0.001
32	HR-106	PoPB/BD2-202	y= 0.036x+1.774	0.277	14.589	<0.001

Rows 1–12, 14–17, 19–28, rows 13, 18, 29–32, and rows 2–3, 5, 10, 12, 14, 16–18, 21–27 show morphometric characteristics that are correlated to both hatching rate (HR) and survival rate (SR), are only correlated to HR, and are negatively correlated to HR, respectively.

APB = anterior part of body; BD-I/BD-II = body depths I and II; BL = body length; HL = head length; PoPB = posterior part of body.

Table 3. Table 3. Simple regression equations, explanatory effect (r^2), F and p values of the significant relationships between the mean and standard deviation of survival rate (at 106, 130, 178, and 202 h postexposure) and morphometric characteristics (at 82, 106, 130, 154, 178, and 202 h postexposure).

No.	Variables			r^2	F	p
	Independent	Dependent	Equations			
1	APB/BD1-82	SR-106	y=9.318x-17.233	0.243	12.199	0.001
2	APB-82	SR-130	y=-50.637x+147.456	0.295	15.933	<0.001
3	APB/HL-106	SR-130	y=30.620x+39.991	0.242	12.165	0.001
4	BL-82	SR_{SD}-130	y=12.202x-23.874	0.251	12.705	0.001
5	BL/BD2-82	SR_{SD}-130	y=3.566x-3.731	0.224	10.955	0.002
6	APB-130	SR_{SD}-130	y=33.155x-29.478	0.217	10.519	0.002
7	BL/APB-130	SR_{SD}-130	y=-23.904x+79.486	0.307	16.836	<0.001
8	BL/PoPB-130	SR_{SD}-130	y=64.618x-88.036	0.282	14.959	<0.001
9	BL/HL-130	SR_{SD}-130	y=-15.635x+80.156	0.318	17.713	<0.001
10	APB/PoPB-130	SR_{SD}-130	y=64.618x-23.418	0.282	14.959	<0.001
11	APB/BD1-130	SR_{SD}-130	y=9.857x-20.775	0.221	10.779	0.002
12	PoPB/HL-130	SR_{SD}-130	y=-20.869x+69.919	0.419	27.376	<0.001
13	APB-82	SR-178	y=-47.663x+143.670	0.281	14.842	<0.001
14	APB/HL-106	SR-178	y=28.498x+43.023	0.225	11.058	0.002
15	BL/APB-178	SR-178	y=33.018x-8.204	0.293	15.751	<0.001
16	BL/PoPB-178	SR-178	y=-116.901x+266.212	0.269	14.007	0.001
17	APB/PoPB-178	SR-178	y=-116.901x+149.311	0.269	14.007	0.001
18	APB/BD1-178	SR-178	y=-17.196x+156.305	0.347	20.177	<0.001
19	BD1/BD2-178	SR-178	y=212.769x-51.069	0.436	29.335	<0.001
20	BL-82	SR_{SD}-178	y=12.518x-24.973	0.255	13.026	0.001
21	BL/BD2-82	SR_{SD}-178	y=3.688x-4.456	0.232	11.458	0.002
22	APB-130	SR_{SD}-178	y=33.696x-30.301	0.217	10.516	0.002
23	BL/APB-130	SR_{SD}-178	y=-24.620x+81.332	0.315	17.497	<0.001
24	BL/PoPB-130	SR_{SD}-178	y=66.618x-91.312	0.291	15.566	<0.001
25	BL/HL-130	SR_{SD}-178	y=-15.858x+80.987	0.317	17.604	<0.001
26	APB/PoPB-130	SR_{SD}-178	y=66.618x-24.693	0.291	15.566	<0.001
27	APB/BD1-130	SR_{SD}-178	y=10.042x-21.541	0.222	10.842	0.002
28	PoPB/HL-130	SR_{SD}-178	y=-21.294x+70.945	0.422	27.748	<0.001
29	BD1/BD2-178	SR_{SD}-178	y=-181.086x+132.195	0.324	18.199	<0.001
30	APB/BD2-154	SR-202	y=35.084x-21.934	0.226	11.115	0.002
31	APB-178	SR-202	y=-70.227x+155.821	0.279	14.680	<0.001
32	BL/APB-178	SR-202	y=55.139x-94.015	0.223	10.892	0.002
33	APB/BD1-178	SR-202	y=-29.084x+182.178	0.270	14.087	0.001
34	PoPB-82	SR_{SD}-202	y=18.943x-22.827	0.251	12.767	0.001
35	BL/PoPB-82	SR_{SD}-202	y=-36.460x+72.632	0.217	10.532	0.002
36	BL/BD1-82	SR_{SD}-202	y=6.930x-41.396	0.330	18.680	<0.001
37	BL/HL-82	SR_{SD}-202	y=25.952x-92.339	0.233	11.547	0.002
38	APB/PoPB-82	SR_{SD}-202	y=-73.956x+59.293	0.236	11.720	0.001
39	APB/BD1-82	SR_{SD}-202	y=20.816x-48.743	0.302	16.477	<0.001
40	PoPB/BD1-82	SR_{SD}-202	y=8.966x-31.872	0.472	33.940	<0.001
41	PoPB/HL-82	SR_{SD}-202	y=15.172x-25.254	0.282	14.921	<0.001
42	BD1-106	SR_{SD}-202	y=-306.699x+130.108	0.458	32.076	<0.001
43	BD2-106	SR_{SD}-202	y=-201.617x+134.980	0.484	35.699	<0.001
44	BL/BD2-106	SR_{SD}-202	y=12.392x-54.872	0.220	10.722	0.002
45	BD1/HL-106	SR_{SD}-202	y=-203.849x+106.885	0.323	18.095	<0.001
46	BD2/HL-106	SR_{SD}-202	y=-108.658x+92.748	0.276	14.451	0.001
47	BL/BD2-154	SR_{SD}-202	y=-8.795x+76.172	0.237	11.819	0.001
48	BL/HL-154	SR_{SD}-202	y=-23.286x+110.853	0.261	13.408	0.001
49	PoPB/BD2-154	SR_{SD}-202	y=-11.512x+66.119	0.268	13.900	0.001
50	PoPB/HL-154	SR_{SD}-202	y=-27.205x+86.438	0.297	16.087	<0.001
51	BD1/BD2-154	SR_{SD}-202	y=-161.830x+117.985	0.261	13.422	0.001
52	BL/BD2-178	SR_{SD}-202	y=-19.190x+159.945	0.294	15.852	<0.001
53	PoPB/BD2-178	SR_{SD}-202	y=-23.251x+130.088	0.253	12.878	0.001
54	BL-202	SR_{SD}-202	y=-30.154x+127.305	0.238	11.860	0.001
55	BL/HL-202	SR_{SD}-202	y=-19.760x+102.959	0.228	11.242	0.002

Rows 1, 12, 18–19, 28–30, 33-36, 38–43, 45–47, 49, 51–52, rows 2–11, 13–17, 20–27, 31–32, 37, 44, 48, 50, 53–55, and rows 2, 7, 9, 12–13, 16–18, 28–29, 31, 33, 35, 38, 42–43, 45–55 show morphometric characteristics that are correlated to both hatching rate (HR) and survival rate (SR), are only correlated to SR, and are negatively correlated to SR, respectively.

APB = anterior part of body; BD-I/BD-II = body depths I and II; BL = body length; HL = head length; PoPB = posterior part of body; SR_{SD} = standard deviation of survival rate.